DEVELOPMENT OF EXPERIMENTAL SETUP AND ANALYSIS USING STAAD. PRO FOR LIGHTLY REINFORCED BEAM-COLUMN JOINT UNDER SEISMIC LOADING

VOON CHET CHIE

CIVIL ENGINEERING
UNIVERSITI TEKNOLOGI PETRONAS
JANUARY 2009

DEVELOPMENT OF EXPERIMENTAL SETUP AND ANALYSIS USING STAAD.PRO FOR LIGHTLY REINFORCED BEAM-COLUMN JOINT UNDER SEISMIC LOADING

VOON CHET CHIE

CIVIL ENGINEERING

UNIVERSITI TEKNOLOGI PETRONAS

JANUARY 2009

Development of Experimental Setup and Analysis Using STAAD.Pro for Lightly Reinforced Beam-Column Joint under Seismic Loading

by

Voon Chet Chie

Dissertation submitted in partial fulfilment of
the requirement for the
BACHELOR OF ENGINEERING (Hons)
(CIVIL ENGINEERING)

Universiti Teknologi PETRONAS
Bandar Seri Iskandar
31750 Tronoh
Perak Darul Ridzuan

CERTIFICATION OF APPROVAL

Development of Experimental Setup and Analysis Using STAAD.Pro for Lightly Reinforced Beam-Column Joint under Seismic Loading

by

Voon Chet Chie

A project dissertation submitted to the
Civil Engineering Programme
Universiti Teknologi PETRONAS
in partial fulfilment of the requirement for the
BACHELOR OF ENGINEERING (Hons)
(CIVIL ENGINEERING)

Approved by,

(Nabilah bt. Abu Bakar)

UNIVERSITI TEKNOLOGI PETRONAS
TRONOH, PERAK
January 2009

CERTIFICATION OF ORIGINALITY

This is to certify that I am responsible for the work submitted in this project, that the original work is my own except as specified in the references and acknowledgements, and that the original work contained herein have not been undertaken or done by unspecified sources or persons.

(VOON CHET CHIE)

ABSTRACT

The recent occurrence of the Sumatran earthquake in December 2004, which caused substantial damages in Malaysia, suggests that the current design codes and practices need to be revisited. This project aims to develop an experimental setup for the testing of a beam-column joint under seismic loading. Analysis is also conducted to predict the structural behaviour of the frame structure under a time-history earthquake data. A three-storey school building in Malaysia is chosen as the case study. The exterior and end joint of the school building is selected and samples of that joint are constructed. An experimental setup is then designed for testing the joint samples. The record of a 2007 Sumatra earthquake which had a magnitude of M_w=8.4 is obtained and used to investigate the time-history response of the school building. A commercial software, STAAD.Pro is used to analyse the response of the school building to the earthquake. The outcome from the analysis indicates that the joint would be able to sustain the maximum moment, shear and axial forces resulting from the earthquake.

ACKNOWLEDGEMENT

This project, conducted in the Civil Engineering Department of Universiti Teknologi PETRONAS, was done with the help and support of many people whom I would like to thank.

Firstly, I would like to express my sincerest gratitude to my Final Year Project supervisor, Ms. Nabilah Abu Bakar. Her continuous motivation and commitment to this project has made it more meaningful and worthwhile. While maintaining her professionalism as a lecturer and supervisor, she also made effort to understand the difficulties and problems which I encountered.

On the same note, I would also like to express my utmost appreciation to my co-supervisor, Dr. Victor Rivera Macam, who was formerly a lecturer at Universiti Teknologi PETRONAS. Under his guidance, I gained a lot in terms of knowledge and experience. Despite his busy schedule, he always allowed some time for our discussions, for which I am extremely thankful. I will always remember his 'Good Luck' statement after every discussion. Special thanks also to Dr. Narayanan Sambu Potty for his advice on the laboratory undertakings.

In conducting this experimental study, a lot of manpower was required. The experiment could not be done successfully without the help and expertise of the laboratory technicians of Civil Engineering and Mechanical Engineering Department who have been very helpful, unconditionally. I would like to take this opportunity to sincerely thank Johan, Meor, Idris, Za'aba, Jani, Hafiz and Zaini.

For the purpose of this experimental study, I also engaged the assistance of several parties. Here, I would like to acknowledge the staffs of BBR Construction Systems (M) Sdn. Bhd. namely Voon Yok Lin, Paul Cheong, Ho Kim Tuan and Patrick Teoh for their tireless effort and assistance in the casting and procurement of concrete specimens. I would also like to extend my thanks to Mr. Ho of Kean Seng Engineering Works for his help in fabricating the steel sections.

Undertaking this project has been a great challenge, physically and mentally. Throughout, my friends have been there to provide support and help. I would like to personally convey my appreciation to Look, Fu Shen, San Yin, Kareen, Leo, Melvin, Shean Chuan, Tzu Fen, Zuraimi, Amri and others who have contributed directly or indirectly to the completion of this project.

Last but not least, my deepest appreciation to my father, mother, brother and sister for their never-ending love, care and patience. I could not have done this without their encouragement and understanding.

TABLE OF CONTENTS

LIST OF TABLES

LIST OF FIGURES

ABBREVIATION

BS	British Standard
M_w	Moment magnitude
UTC	Universal Time Coordinated
σ	Stress / Force per unit area (Pa or N/mm^2)
ε	Strain (deformation per unit length)
COSMOS	Consortium of Organizations for Strong-Motion Observation Systems

CHAPTER 1
INTRODUCTION

This chapter will elaborate in details the background that lead to this study, the problem statement and also the objectives and scope of this study.

1.1 Background of Study

Malaysia is geographically blessed to be located a distant away from high seismic regions. The nearest fault lines or active seismic sources in Sumatra, which is about 350km away from Peninsular Malaysia, is considered relatively far away. This classifies Malaysia in the category of 'low seismic hazard' (Megawati, et al., 2005).

On 26^{th} December 2004, an earthquake with magnitude of 9.1 on the Richter scale occurred in the Indian Ocean, off the west coast of Sumatra. The tremors from the earthquake were reported in several states along the west coast of Peninsular Malaysia. Several recurrences that followed after the 26^{th} December earthquake were also felt. This experience brought forward and instilled some alertness in the public that Malaysia is not totally safe from earthquakes.

In actual truth, Malaysia has been experiencing tremors as a result of earthquakes in nearby regions. Table 1.1 shows the data taken from the Malaysian Meteorological Department's (MMD) official website showing record of earthquakes in Malaysia dating back to 1909. The intensity of the recorded earthquakes, measured according to the Modified Mercalli Scale, is explained in details in Appendix A.

Table 1.1 Earthquakes felt in Malaysia (Source: Malaysian Meteorological Department (MMD) Official Website, http://www.kjc.gov.my/home_e.html)

State	Frequencies	Maximum Intensity Observed (Modified Mercalli Scale)
Peninsular Malaysia (1909 - September 2007)		
Perlis	2	IV
Kedah	13	V
Penang	36	VI
Perak	22	VI
Selangor/Kuala Lumpur	46	VI
Negeri Sembilan	7	V
Melaka	15	V
Johor	27	VI
Pahang	7	III
Terengganu	1	IV
Kelantan	3	IV
Sabah (1923 - September 2007)		
Sabah	27	VII
Sarawak (1923 - September 2007)		
Sarawak	5	V

A rough glance at the figures shows some coherence, that is several states along the west coast of Peninsular Malaysia – Selangor/Kuala Lumpur, Penang, Johor, and Perak have the highest frequencies of earthquakes. Coincidently, these are also the most developed states in the country, with a significant number of old and new buildings being built over the last decade. Despite charting a high growth in the construction of new buildings, these states are now at the highest risk during the occurrence of an earthquake.

In view of the safety of structures subjected to earthquakes, the Town and Country Planning Department and various related parties have commenced work to draft out guidelines that will ensure the future safety of buildings in Malaysia. As the study of earthquake on buildings is a relatively new field in Malaysia, continuous researches and experiments need to be conducted to assess the impacts.

1.2 Problem statement

Most of the buildings in Malaysia use concrete as its main material for construction. This is backed up by the fact that Malaysia has an abundance of raw materials required to make concrete.

In a recent study by Mansor et al. of the Malaysian Public Works Department (PWD) and Universiti Teknologi Malaysia (UTM), it has been clarified that the existing design code adopted by engineers for buildings in Malaysia does not incorporate seismic effects. For the design and detailing of reinforced concrete (RC) structures, engineers have been using *BS 8110 'Structural use of concrete'*. RC designs done in accordance to BS 8110 are considered lightly reinforced. Since most RC structures in Malaysia are based on this code, the vulnerability to earthquake risk is very high.

In papers by Lowes and Altoontash (2003) and Pantelides et al. (2008), the authors found out that most post-earthquake structural collapses could be attributed to joint failure. Thus, in order to design a building to withstand earthquake loading, emphasis on its joint detailing would be very crucial. The structures of RC buildings in Malaysia are designed as lightly reinforced. Since the extend of earthquake loading in Malaysia is slightly different as compared to other countries in high-seismic zones, a more practical study on the joint behaviour should be carried out. The study should be oriented towards the Malaysian earthquake scenario.

1.3 Objectives and Scope of Study

While previous studies done by the PWD indicate that the buildings in Malaysia are still safe for occupancy, the reports of cracks in several buildings indicate otherwise. In an article by *The Star* dated 13th September 2007, the local print media reported minor cracks appearing in a hospital block in Kuala Lumpur after an earthquake struck Sumatra. Therefore, generally this research is specifically meant to investigate the effects of earthquake loading on RC buildings in Malaysia.

To date, limited experiments have been conducted to investigate the behaviour of RC structures subjected to earthquake forces in Malaysia. Through this study, the author intends to further investigate the characteristics of lightly reinforced concrete joints in structures by conducting experimental studies.

In short, the objectives are as follows.

- Designing an experimental setup for the testing of a selected beam-column joint.
- Analysing the effects of a Sumatran earthquake to the structure using STAAD.Pro to find out the response of the structure.

The scope of work would cover the following:-

- The structure analysed is a school building designed by Malaysia Public Work Department (JKR).
- The project would only involve designing experimental setup for the testing of the concrete joints.
- Using STAAD.Pro, time-history analysis of Sumatra 2007 earthquake will be used to analyse its effect to the structure.

CHAPTER 2
LITERATURE REVIEW

2.1 Inelastic Property of Concrete Subjected to Repetitive Loads

The main problems associated with concrete structures during earthquakes are bending deformation and also shear force generated due to dynamic deformation (Tatsuo (ed.) 1997). Concrete loses its resistance and stiffness when it is subjected to high repetitive stress in the plastic zone. Figure 2.1 below shows the stress-strain curve of concrete and the variation of tangent elasticity modulus, E_t which represents stiffness.

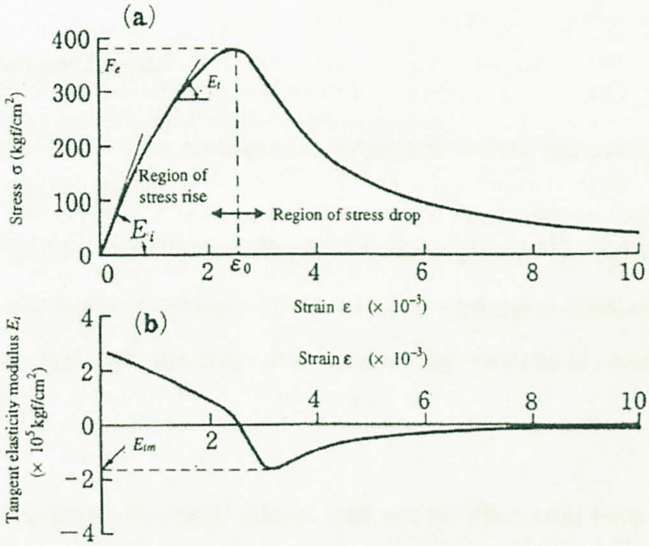

Figure 2.1. (a) σ - ε curve and (b) E_t – ε curve due to static loading (Source: Tatsuo, 1997)

As the strain in concrete increases, the stiffness gradually decreases. Quoting Tatsuo (ed.) (2008),

> "A peak stress point is observed when the strain is in the range of 1.5×10^{-3} - 2.5×10^{-3}. After this, stress begins to reduce, indicating negative stiffness."

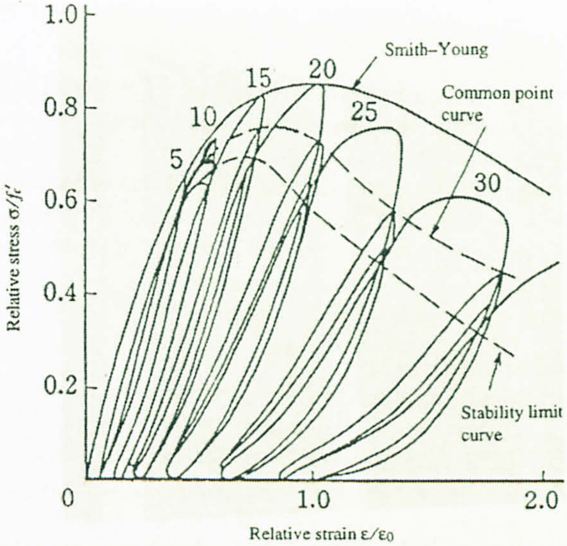

Figure 2.2. $\sigma - \varepsilon$ curve envelope under repetitive loading.
(Source: Tatsuo (ed.), 1997)

The stress-strain curve envelope under repetitive loading also shows similar pattern as the curve envelope under static loading.(Refer Figure 2.2)

2.2 Beam-Column Joints

In an incidence of an earthquake, structural failure may occur in 2 modes as described by Erdey (2007):-

- *Overall failure* – involves collapse or overturning of the entire structure.
- *Component failure* – failure of one or more structural elements, mostly joints, due to a type of damage that makes the structural component or joint unusable.

The mechanism of overall failure will not be discussed here. More details on component failure, particularly in joints, will be explained. Figure 2.3 shows the joint degradation of a concrete structure.

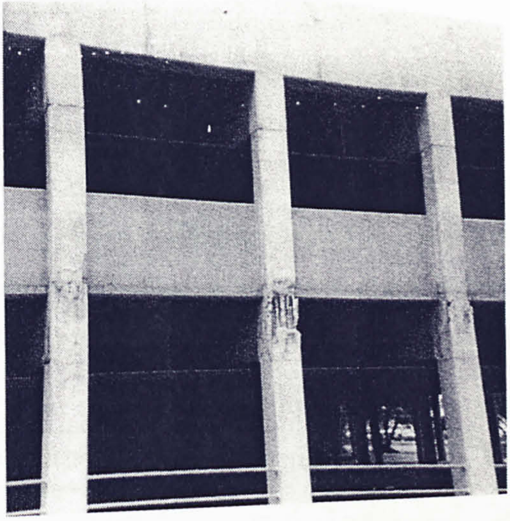

Figure 2.3. Initial stages of column joint degradation in the progressive failure of a fashion center parking structure in the Whittier Narrows earthquake, 1987. (Source: Erdey, 2007)

Erdey (2007), on his explanation of the failure of the fashion center parking structure, described:-

> "...during each aftershock, the large, rapidly reversed horizontal shear forces produced a grinding action at the beam-column joint that pulverized the concrete until it totally disappeared. Once the concrete was gone, the slender rebars, lacking lateral confinement, could no longer support the weight of the massive concrete floor structure and buckled."

In a study by Laura and Altoontash (2003) and Pantelides et al. (2008), they reported that RC buildings constructed before the 1970s had beam-column joints with no steel hoops provided at the joint region. The consequence of this orientation was serious stiffness and strength loss. Also, longitudinal bars had insufficient anchorage passing through or terminating in the joint. In certain cases, the building joints designed according to older standards were found to be insufficient, thus resulting in the damage or collapse of the structure during earthquakes. Another beam-column joints failure reported by the authors was due to the pullout of the bottom steel reinforcement at the joint which was not embedded sufficiently into the column. Pantelides et al. (2008) also reported a reduction in bond strength for longitudinal bars with relatively large diameter passing through a column of relatively small depth.

2.3 Earthquakes

Worldwide, earthquakes are being monitored round the clock by various seismic agencies such as the United States Geological Survey (USGS) and Earthquake Engineering Research Institute (EERI). Continuous monitoring has enabled us to draft out a global incidence map of previous seismic events. This has helped in the prediction of earthquakes and consequently the reduction in casualties and damages. The following Figure 2.4 shows the global seismic activities to date.

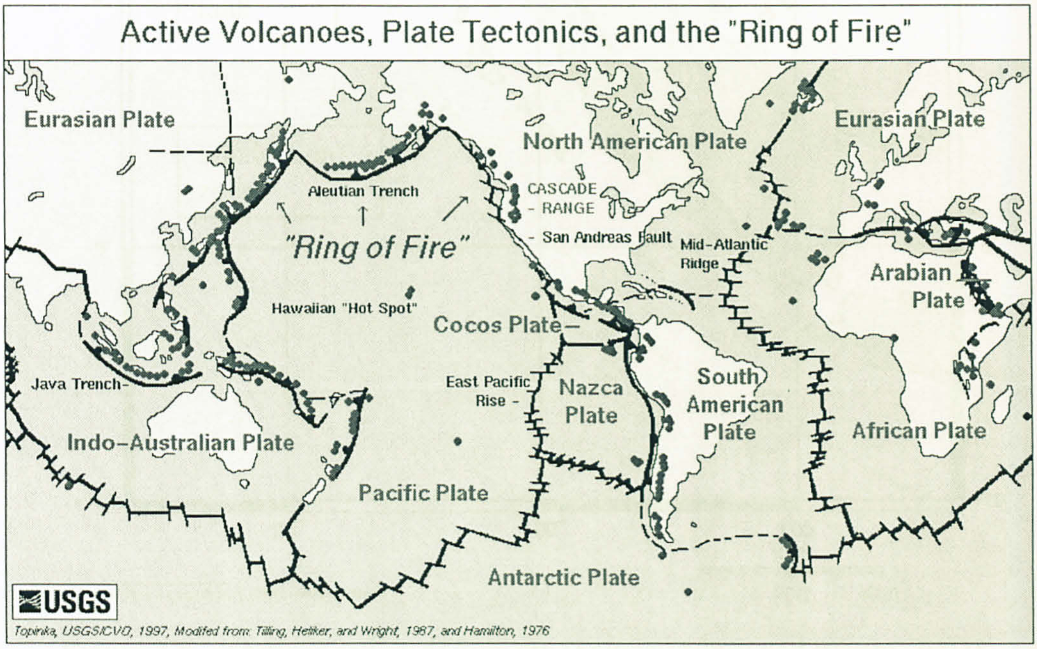

Figure 2.4. The active volcanic and earthquake zones.

In Malaysia, we are indirectly affected by the Sumatran seismic zone which consists of 2 sources, the Sumatran fault and the Sumatran subduction zone (Refer to Figure 2.5). While the Sumatran fault is only capable of producing earthquake magnitudes of not more than 7.8, the Sumatran subduction zone however has a higher magnitude potential (Megawati, et al.,2005). The highest magnitude recorded due to the Sumatran subduction was in 1833 with a magnitude of 8.8-9.2 (Adnan and Irsyam, 2002). As Kuala Lumpur is located at about 500km away from the subduction zone, this would mean that an earthquake with magnitude M_w=8.5 would result in devastating ground motions. It was estimated that the recurrence interval of the 1833 incident was 265 years.

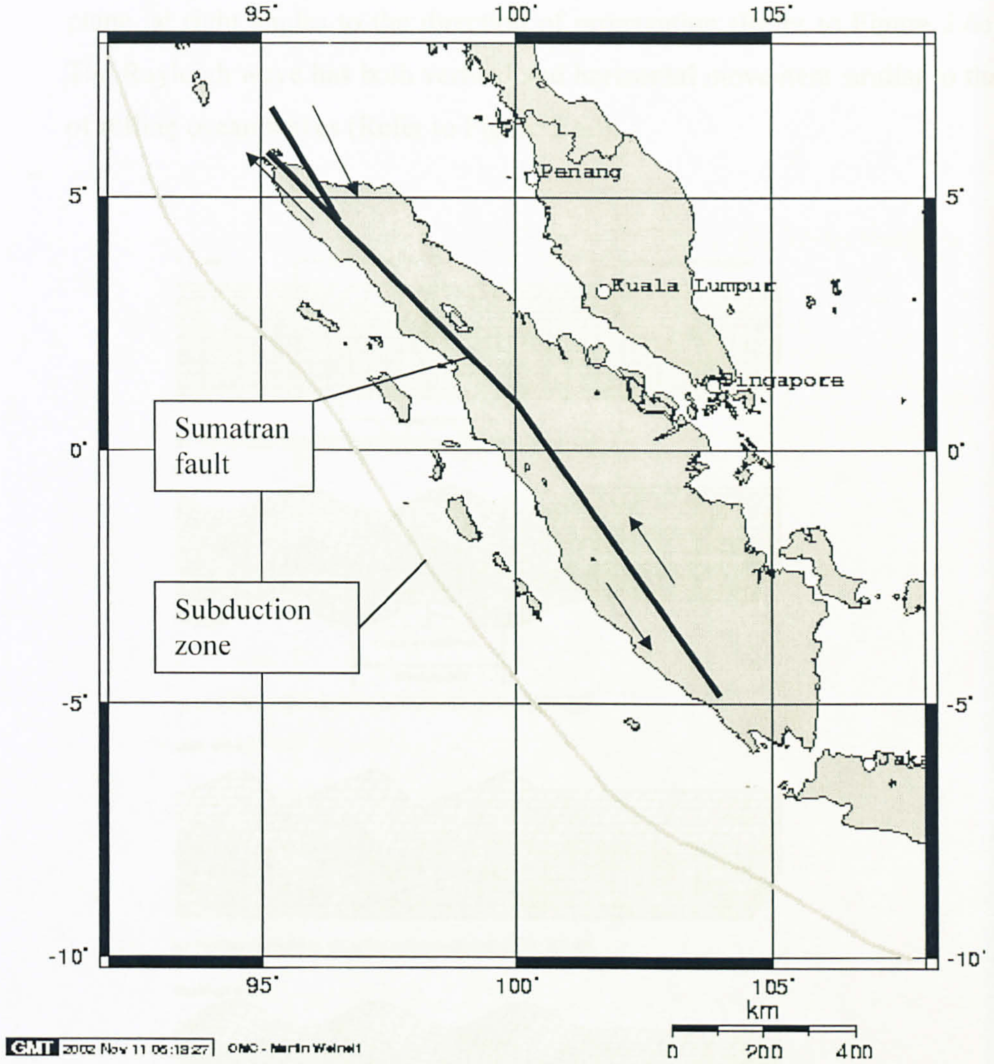

Figure 2.5. Tectonic setting of Sumatra (Source: Adnan and Irsyam, 2002)

Bolt (2003), in his work described that earthquakes can be associated with 3 types of elastic waves:-

- Primary or P wave – It is the faster of the waves and propagates with a motion similar to that of sound, i.e. it compresses and dilates the rock. This wave can travel through both solid rock and liquid material (Refer to Figure 2.6a).
- Secondary or S wave – It is the slower wave and cannot be transmitted through liquid. When it propagates, it shears the rock sideways at right angles to the direction of travel. (Refer to Figure 2.6b)
- Surface wave (Love & Rayleigh wave) – The Love wave is almost similar to that of the S wave, however it moves the ground sideways in a horizontal

plane, at right angles to the direction of propagation (Refer to Figure 2.6c). The Rayleigh wave has both vertical and horizontal movement similar to that of rolling ocean waves (Refer to Figure 2.6d).

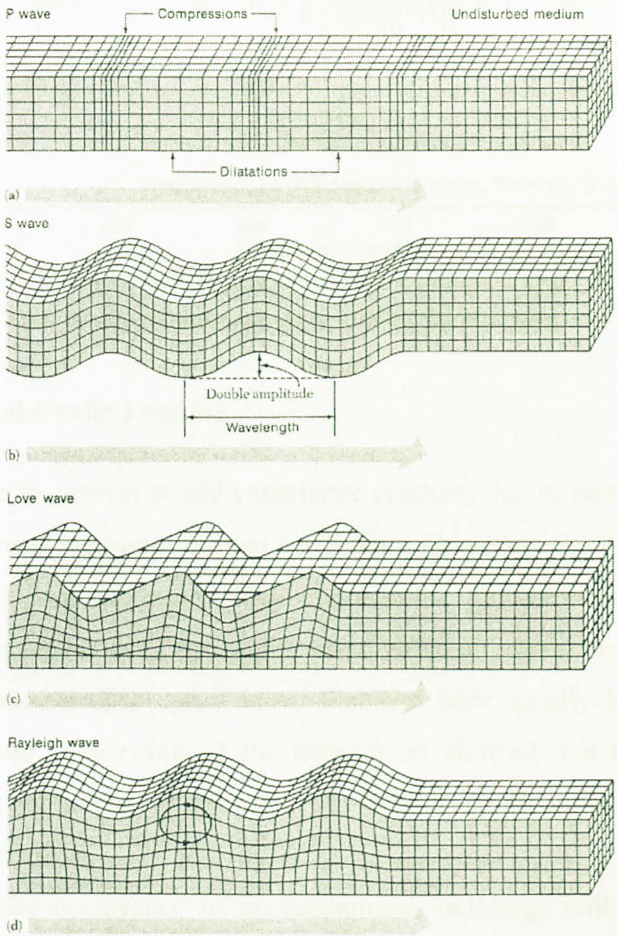

Figure 2.6. Ground motion near the ground surface in four types of earthquake waves. (Source: Bolt, 2003)

Earthquakes are difficult to measure and can only be detected by electronically sensitive equipments called seismograph. These equipments produce graphs called seismogram that show the ground motion at a measuring station. In general, a seismogram of an earthquake has certain characteristics. It shows the arrival time of the P-waves, S-waves, and surface waves. The following Figure 2.7 shows an example of a seismogram.

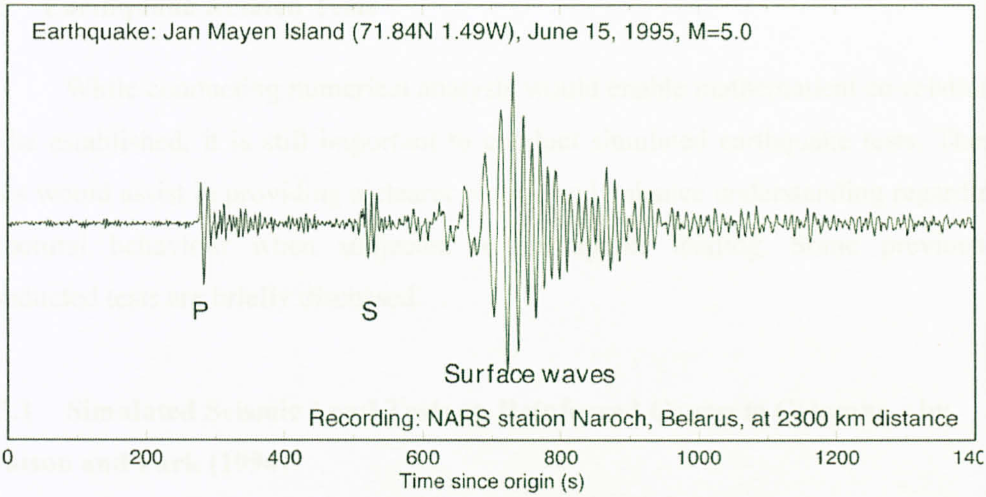

Figure 2.7 The seismogram of an earthquake
(Source:chuma.cas.usf.edu/~juster/A2/seismogram.gif)

2.4 Cracks and Cyclic Loading

Concrete in general would experience cracking due to numerous factors such as shrinkage, creep, deformation and settlement. However, BS 8110 has taken into account the allowance for certain crack widths in the design of concrete structures. In a paper by Walraven (1994), the author highlighted an experiment that investigated the effect of flexural shear on a beam that had been axially loaded earlier until cracking occurred. The result of the experiment showed that the vertical cracks across the cross section of the beam did not have a significant effect on the flexural strength of the beam.

During the occurrence of an earthquake, buildings will be subjected to a repeated loading-unloading process call cyclic loading. The force induced on the building is caused by the building's relative movement to the ground acceleration. The paper by Walraven (1994) stated that there is difference in strength of concrete between the first and subsequent loading cycles.

> " ...This can be explained by the irreversible damage to the cement matrix...any new cycle of loading leads to further damage of the crack faces, resulting in steadily increasing values of the shear displacement and the crack width at peak loading"
> (Walraven, 1994)

2.5 Earthquake Related Tests

While conducting numerical analysis would enable mathematical co-relations to be established, it is still important to conduct simulated earthquake tests. These tests would assist in providing a clearer picture and enhance understanding regarding structural behaviour when subjected to earthquake loading. Some previously conducted tests are briefly discussed.

2.5.1 Simulated Seismic Load Tests on Reinforced Concrete Columns – by Watson and Park (1994)

Watson and Park (1994) carried out simulated seismic load tests on RC columns with various quantities of transverse reinforcement to obtained more suitable equations for the design of transverse reinforcement. 11 RC columns, each 3.9m high with 400mm square or octagonal cross section were subjected to low, moderate or high axial compressive loads and to reversible quasi-state lateral loads that resemble severe earthquake loading (Refer to Figure 2.8). Reference is made to the American (ACI 318-89) and New Zealand (NZS 3101) code for the detailing of the reinforcements. (Refer to Figure 2.9)

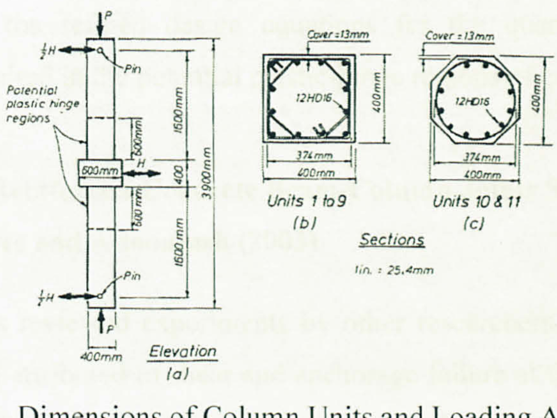

Figure 2.8. Dimensions of Column Units and Loading Arrangements (Source: Watson and Park, 1994)

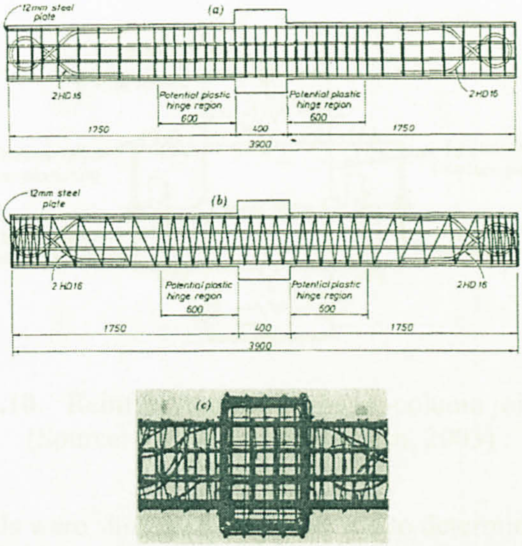

FIG. 2. Arrangement of Reinforcement in (a) Square Column Units; (b) Octagonal Column Units; and (c) Central Stub

Figure 2.9. Reinforcement detailing (Source: Watson and Park, 1994)

The reversible quasi-static load was applied at the mid-height of the column through a loading frame by a hydraulic jack. A universal testing machine was used to apply the axial compressive load at each end of the column.

It was found that the design charts adopted for ductility gave a more satisfactory prediction of column behaviour but yet conservative predictions. Hence, the derivation of the refined design equations for the quantities of confining reinforcement (required in the potential plastic-hinge regions of columns) is justified.

2.5.2 Modeling Reinforced-Concrete Beam-Column Joints Subjected to Cyclic Loading – by Lowes and Altoontash (2003)

The authors reviewed experiments by other researchers and found out that joint failure can be attributed to shear and anchorage failure at the joints. They then developed a model to represent the response of reinforced-concrete beam-column joints under reversed cyclic loading. The joint model explicitly represents the mechanisms that may determine inelastic joint action through the combined action of one-dimensional shear panel, bar-slip and interface-shear components. It is a four-node, 12-degree-of-freedom element that can be use in two-dimensional nonlinear analysis of RC structures. The model is showed in Figure 2.10.

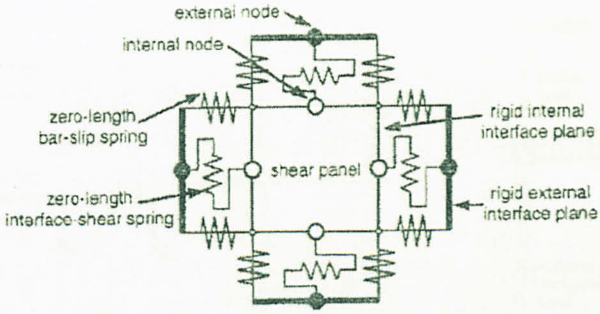

Figure 2.10. Reinforced concrete beam-column joint model
(Source: Lowes and Altoontash, 2003)

Several models were simulated and observed to determine the response of the proposed model. Through the results, it can be concluded that the proposed model represents the fundamental characteristics of response for joints subjected to moderate shear forces.

2.5.3 Seismic Rehabilitation of Reinforced Concrete Frame Interior Beam-Column Joints with FRP Composites - by Pantelides, et al. (2008)

The authors conducted an experimental research to investigate the usage of carbon fiber-reinforced plastic (CFRP) for seismic rehabilitation of RC interior beam-column joints. CFRP was aimed at improving storey shear capacity, displacement ductility, energy dissipation and inelastic rotation capacity of the joint under simulated seismic load.

The research is based on the understanding that RC buildings constructed before 1970s have beam-column joints with insufficient shear strength. This fact becomes even more significant when several building collapses due to inadequate joint confinement were reported during earthquakes.

Pantelides, et al. tested 2 types of beam-column joints; Type I had a beam 406mm wide and 610mm deep, while Type II has a beam 406mm wide and 406mm deep. Both types had a column with dimensions 406x406 mm. The detailing of the reinforcement followed older standards like the ACI Building Code Requirements for Reinforced Concrete 318-63 (ACI 1963). The experimental setup is as shown in Figure 2.11.

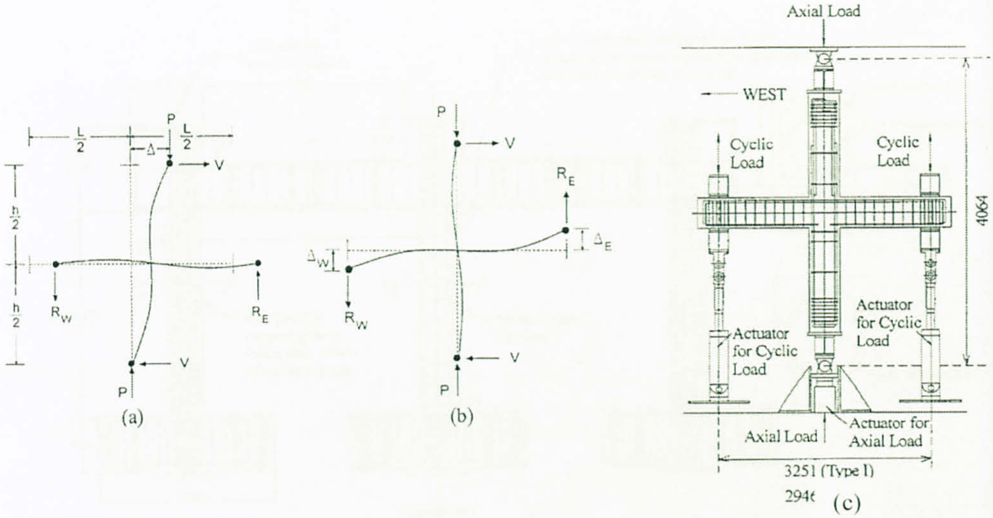

Figure 2.11. (a) Idealized joint; (b) joint tested in the laboratory; (c) experimental setup of beam-column test (Source: Pantelides, et al., 2008)

The end result of the experiment showed that CFRP was successful in promoting ductile behaviour by delaying brittle joint shear failure and pullout of the beam bottom steel bars at the joint.

2.5.4 Dynamic Shear and Axial-Load Failure of Reinforced Concrete Columns – by Elwood and Moehle (2008)

The authors conducted an experimental research using shaking table tests to investigate the behaviour of a frame subjected to simulate earthquake motion. The global response of the frames and the shear and axial-load response are discussed in the paper. Figure 2.12 shows the specimen that was tested.

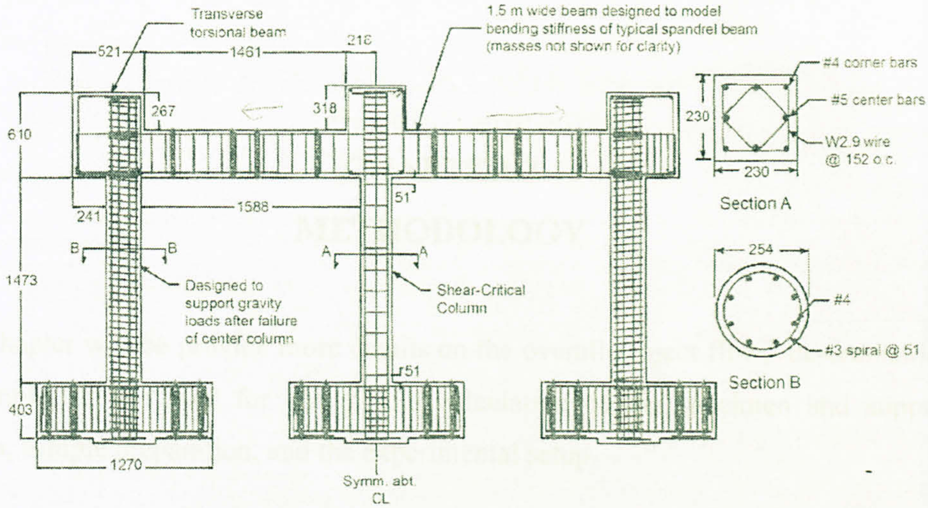

Figure 2.12. Shaking table test specimen by Elwood and Moehle.
(Source: Elwood and Moehle, 2008)

Quoting Elwood and Moehle (2008), "Shaking table tests were designed to observe the process of dynamic shear and axial-load failures in reinforced concrete columns when an alternative load path is provided for load redistribution." The centre column was designed to undergo shear and axial load failure during testing by having wide spacing of transverse reinforcement. Theoretically, the shear and axial load would then be redistributed to the 2 outer columns.

Column axial-load stresses were simulated by adding introducing 31,000 kg of mass (equivalent to a seven-storey building). The additional axial load needed to induce failure in the centre column was achieved using a pneumatic jack.

The result from the experiment showed that redistribution of loads happens during shear and axial-load failure of a reinforced concrete column. This could be observed from the sudden dynamic amplification of the axial loads transferred to the outer columns as the centre column failed.

CHAPTER 3
METHODOLOGY

This chapter will be provide more details on the overall project flow, determination of sample, theory used for design and calculation of the specimen and support system, sample preparation, and the experimental setup.

3.1 Project Flow Chart

Generally, this research can be divided into 2 different stages; Stage 1 and Stage 2. Pre-experimental works are done in Stage 1 and covers literature review, developing experimental setup, design of specimen, support system, and testing jig, and seeking quotation from suppliers.

Setting of experimental works are done in Stage 2 and involves procurement of materials, setting up of experiment, software analysis using STAAD.Pro, results and discussion, conclusion, and the completion of this research. The summary of project flow is as shown in Figure 3.1.

Literature Review

↓

Develop experimental setup

↓

Obtain data of time-history of an earthquake

↓

Analyse time history response of a structure due to the earthquake

↓

Results and discussion

Figure 3.1. Summary of project flow

3.2 Developing Experimental Setup

The following will explain the process of selecting the joint sample, estimating the joint capacity, and the steps used for the design of the support system.

3.2.1 Selection of Sample

Choosing a school building as a case study, the design of the structure is reviewed. The design had been done by the Malaysia Public Works Department (PWD) in 1991. This case study is suitable in this context due to the design standard which was based on BS 8110:1985. The first step required was to select a joint to be investigated. An external beam-column joint as shown in Figure 3.2 was selected due to constraints of the testing equipment. The structural drawing of the building is available in Appendix B

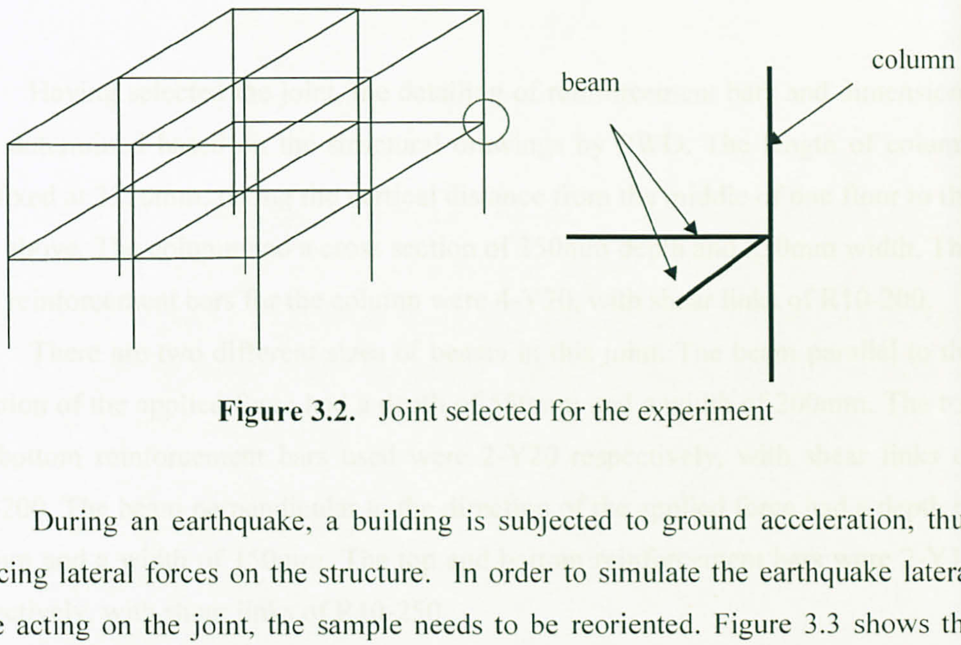

Figure 3.2. Joint selected for the experiment

During an earthquake, a building is subjected to ground acceleration, thus inducing lateral forces on the structure. In order to simulate the earthquake lateral force acting on the joint, the sample needs to be reoriented. Figure 3.3 shows the proposed orientation of the joint sample to be tested.

The selected joint is rotated 90° for several reasons:-

1) The apparatus is only limited to applying force in the vertical direction. There are no other apparatuses available in-house to simulate the horizontal force.
2) No specific mounting frame was fabricated in order hold the column in its

actual position. It was more economical to utilize available apparatuses and fabricate lesser new ones.

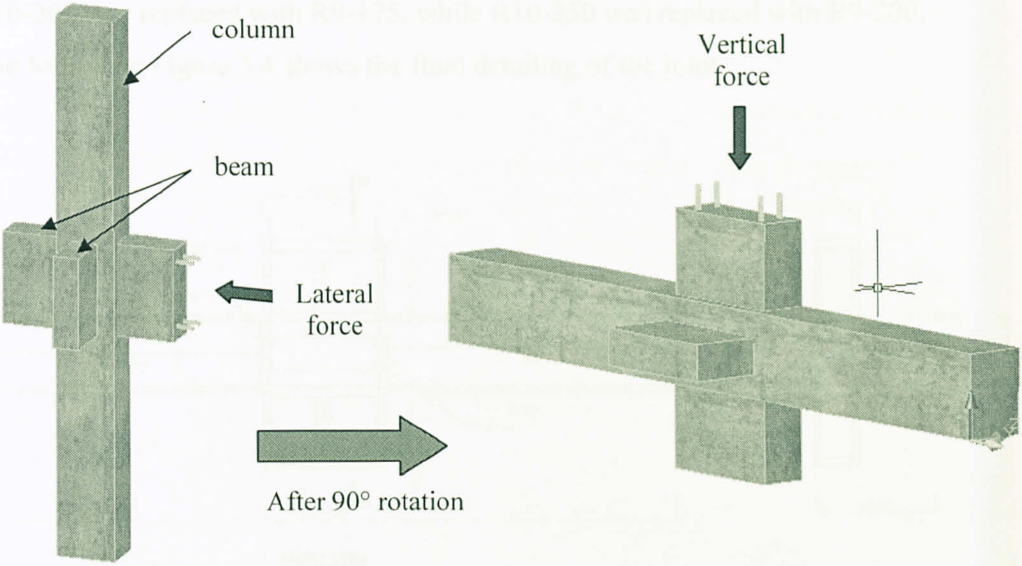

Figure 3.3. Proposed orientation of the beam-column joint for testing.

Having selected the joint, the detailing of reinforcement bars and dimensions were determined based on the structural drawings by PWD. The length of column was fixed at 3250mm, taking the vertical distance from the middle of one floor to the floor above. The column had a cross section of 350mm depth and 250mm width. The main reinforcement bars for the column were 4-Y20, with shear links of R10-200.

There are two different sizes of beams in this joint. The beam parallel to the direction of the applied force had a depth of 550mm and a width of 200mm. The top and bottom reinforcement bars used were 2-Y20 respectively, with shear links of R10-200. The beam perpendicular to the direction of the applied force had a depth of 550mm and a width of 150mm. The top and bottom reinforcement bars were 2-Y16 respectively, with shear links of R10-250.

Besides the two beams mentioned earlier, a third beam was also introduced, having a depth of 550mm and width of 200mm. The purpose of introducing this beam was to act as a restraint for the joint (from the top) and also to provide a surface for applying the load. The beam would have similar reinforcement details as the other beam with similar dimensions; however, this end of the beam would have its reinforcement protruding out and threaded to facilitate connection with the testing apparatus. All R10 bars used as shear links were replaced with R9 bars and spaced at an equivalent spacing because of the unavailability of R10 bars at the time of casting. R10-200 was replaced with R9-175, while R10-250 was replaced with R9-200.

The following Figure 3.4 shows the final detailing of the joint.

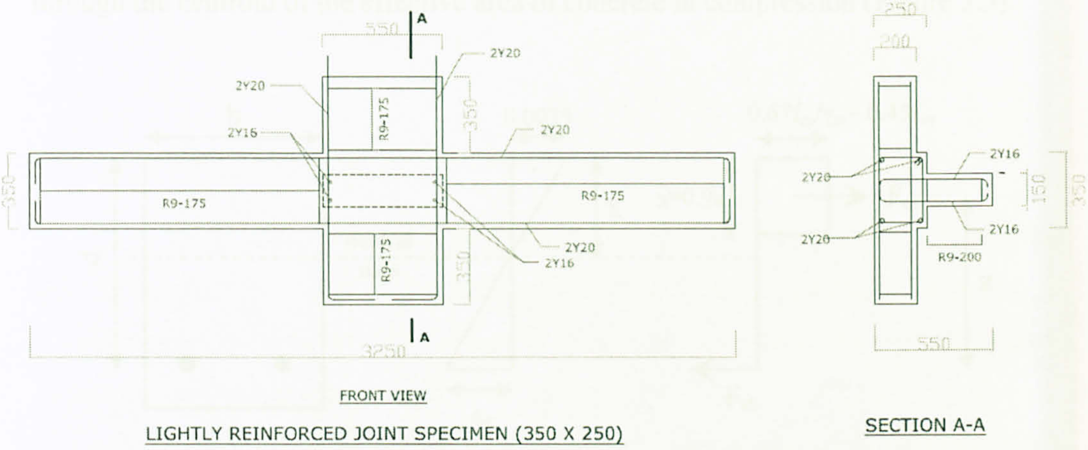

Figure 3.4. Lightly reinforced joint detailing

3.2.2 Estimating joint capacity

Based on the proposed orientation of the beam-column joint, it can be assumed that the column would now behave as a beam. The beam, which acts as a restraint and also gives strength to the joint, is ignored in the computation of the joint capacity. Given the dimensions of the column and the reinforcements, the capacity of the joint can be estimated.

- Concrete grade = 30N/mm^2
- Depth, H = 350mm;
- Width, B = 250mm;
- Cover = 40mm;
- Reinforcement bar strength, f_y = 410N/mm^2 / 460N/mm^2 / 500N/mm^2
- Area (Ø20mm rebar), A_s = 314mm^2

Since all samples were out-sourced, there was a possibility that the contractor replaced the Y-type bars with the T-type bars due to difficulty in obtaining the Y-type bars. Three types of bar strengths were used in the estimation of the joint capacity. The column was assumed to be a singly reinforced rectangular section in bending. Bending of the section will induce a resultant tensile force F_{st} in the reinforcement steel and a resultant compressive force in the concrete F_{cc} which acts through the centroid of the effective area of concrete in compression (Figure 3.5).

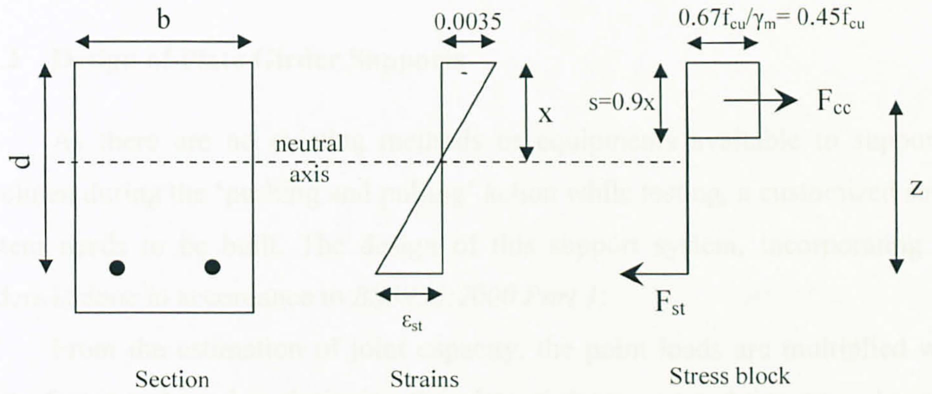

Figure 3.5. Singly reinforced section with rectangular stress block

For equilibrium, the compressive force in the concrete should be balanced by the tensile force of the reinforcement.

$$F_{cc} = F_{st}$$

$$0.45f_{cu}bs = 0.95f_yA_s$$

The moment of resistance of the section is given by,

$$M = F_{st}\ x\ z$$

Since the loading that will be applied on the joint samples during testing will be a point load, the moment of resistance computed should be converted to an equivalent point load by the formula:-

Bending moment due to point load acting at centre span, $M = \dfrac{PL}{4}$

Point load, $P = \dfrac{4}{L}M$

Detailed computation for the estimation of joint capacity is shown in Appendix C. Table 3.2 summarizes the computation of the joint capacity.

Table 3.1. Joint capacity

Bar strength, f_y (N/mm^2)	Moment of resistance (kNm)	Equivalent point load (kN)
410	64.52	79.41
460	71.17	87.59
500	76.31	93.92

3.2.3 Design of Plate Girder Supports

As there are no existing methods or equipments available to support the specimen during the 'pushing and pulling' action while testing, a customized support system needs to be built. The design of this support system, incorporating plate girders is done in accordance to *BS5950:2000 Part 1.*

From the estimation of joint capacity, the point loads are multiplied with a safety factor and used in designing the plate girder support. After several trial and errors, the following dimensions were determined for the plate girder design. The detailed calculation can be referred to in Appendix D. The Figures 3.6 and 3.7 are the cross-section and isometric views of the 1255mm x 200mm x 100mm plate girders.

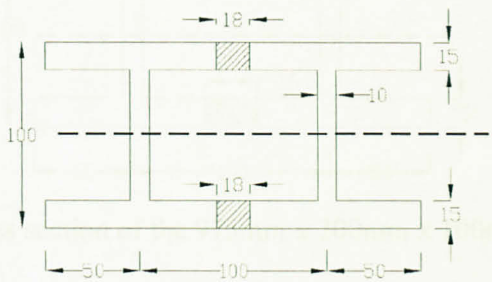

Figure 3.6. Cross-section of the 1255mm x 200mm x 100mm plate girder

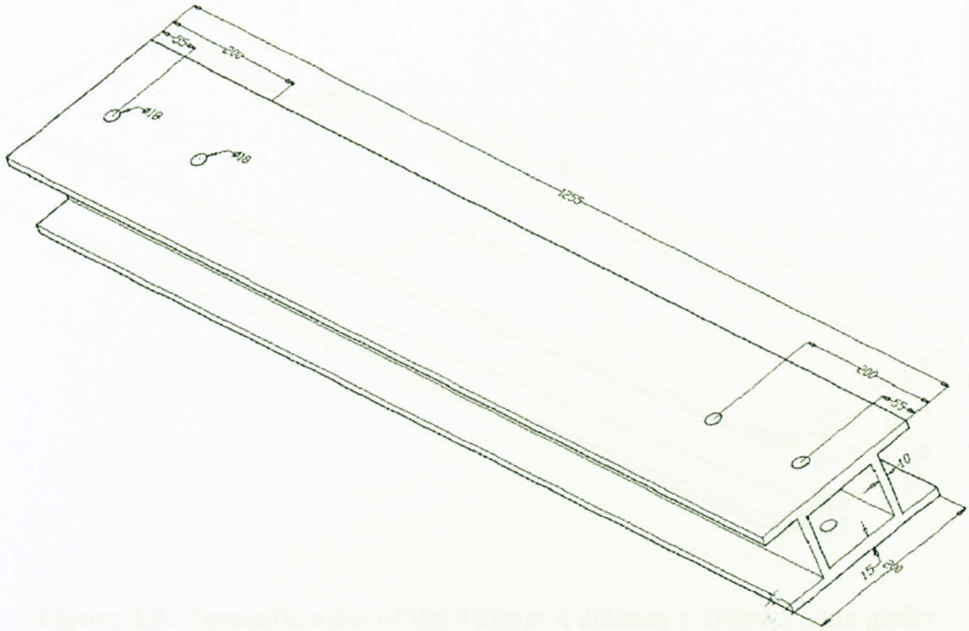

Figure 3.7. Isometric view of the 1255mm x 200mm x 100mm plate girder

Figures 3.8 and 3.9 shows the cross-section and isometric view of the 975mm x 200mm x 100mm plate girder.

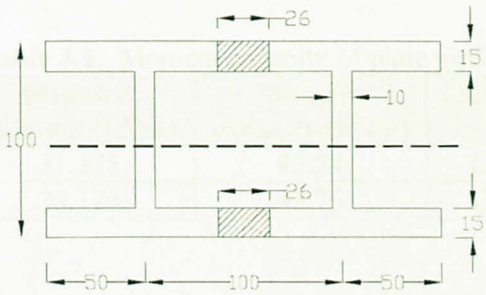

Figure 3.8. Cross section of the 975mm x 200mm x 100mm plate girder

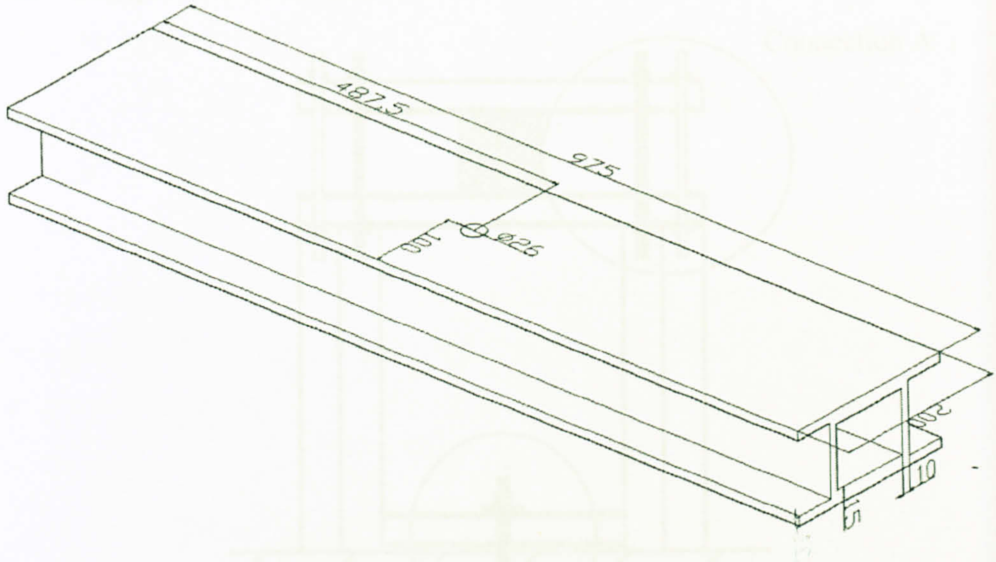

Figure 3.9. Isometric view of the 975mm x 200mm x 100mm plate girder

The use of the plate girders will be shown in the following chapters. Table 3.3 summarizes the estimated moment capacity of the plate girders. It can be seen that the plate girders are designed to have additional capacity and would not fail even though the concrete joint samples have reach their ultimate capacity.

Table 3.2. Moment capacity of plate girders

Plate girder section	Imposed moment (kNm)	Moment capacity (kNm)	Status	Additional capacity (%)
1255 x 200 x 100	31.375	45.54	OK!	+31.1
975 x 200 x 100	24.375	43.73	OK!	+44.3

3.2.4 Design of Bolted Connection

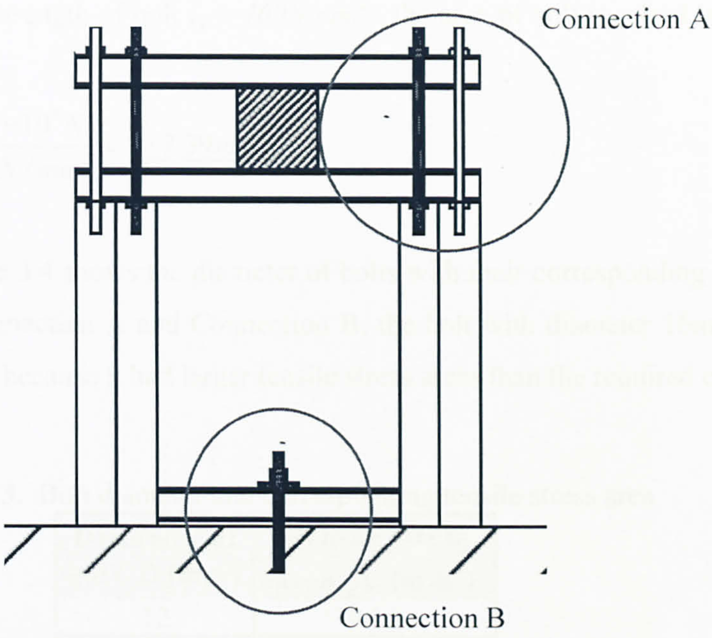

Figure 3.10. Connection detail of support system

In order to attach the support system together, bolts and nuts are used. The design for the connections is done in accordance to *BS5950:2000 Part 1*.

Connection A

Based on the highest point load acting on the support of 93.92kN (assume 100kN), the area of bolt required to sustain the tension force can be calculated. Taking the tension strength of bolt, $f_y = 460N/mm^2$, the force acting per bolt is,

$$F = \frac{100}{4} = 25kN$$

Therefore, the area of bolt required is given by,

$$A_{s,req} = \frac{25 \times 10^3 N}{460N/mm^2} = \underline{54.35mm^2}$$

Connection B

Taking the tension strength of bolt $f_y = 460N/mm^2$, the area of bolt required is given by,

$$A_{s,req} = \frac{100 \times 10^3 N}{460 N / mm^2} = \underline{217.39 mm^2}$$

The following Table 3.4 shows the diameter of bolts with their corresponding tensile stress area. For Connection A and Connection B, the bolt with diameter 16mm and 24mm was selected because it had larger tensile stress areas than the required one.

Table 3.3. Bolt diameter and corresponding tensile stress area

Diameter of bolt, D (mm)	Tensile stress area, A_t (mm^2)
12	84.3
16	157
20	245
22	303
24	353
27	459
30	561

3.2.5 Experimental Setup

The experiment involves the use of a dynamic actuator with a capacity of 2000kN, mounted on a universal frame (refer to Figure 3.11). The following facilities are located at the Civil Engineering Laboratory of Universiti Teknologi PETRONAS

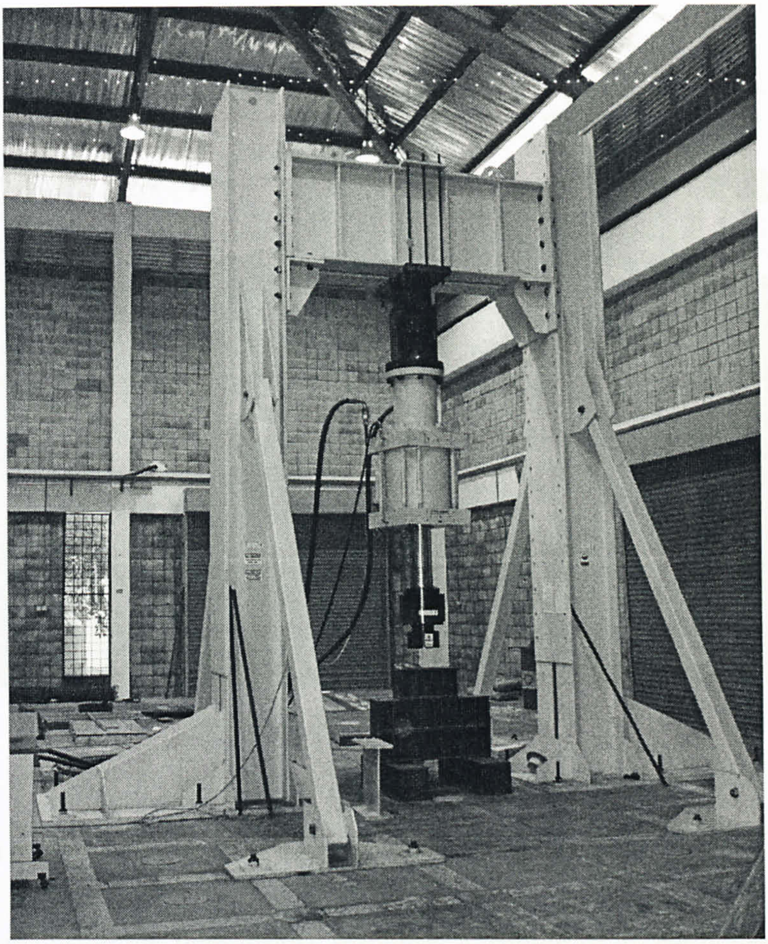

Figure 3.11. Dynamic actuator mounted on a universal frame

The universal frame is fixed onto a strong floor, with voids at every 1 m interval. These voids in the floor will be utilized to secure the support system for the joint sample onto the ground as shown in Figure 3.12. The sample of the beam-column joint is then secured down to the supports by means of bolts and plate girders to prevent it from movement. Stiffened plate girders are used as the supports, supporting the sample at 2 points.

To lift the sample onto the support, a 10 tonne gantry crane will be used along with a forklift. On each sample, 2 hooks have been casted in to act as lifting points. Once the sample has been placed on the supports, the test jig will then be bolted on to the joint. The test jig can also be connected to the actuator by using bolts.

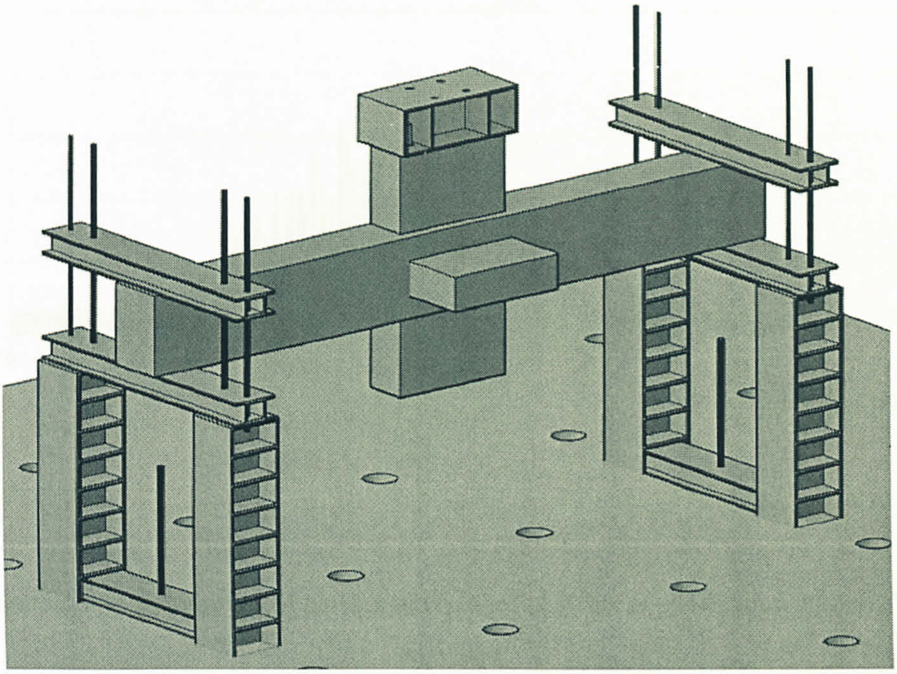

Figure 3.12. Experimental setup

3.3 Data of Time-History for Sumatra 2007 Earthquake

In analysing the time-history response, a sample of an earthquake data was obtained from the Consortium of Organizations for Strong-Motion Observation Systems (COSMOS) Virtual Data Center website. COSMOS is a non-profit organization aimed to create awareness for earthquake safety. It provides free acquisition and application of strong-motion data to users.

The time history data of an earthquake recorded in Southern Sumatra on 12th September 2007 at 11.10 UTC was chosen. The epicentre is located at -4.52 in latitude and 101.374 longitude, with the depth of 34km. The earthquake had a magnitude of M_w=8.4 and was recorded by the Sikuai Island station located West of Sumatra. Figure 3.13 shows the seismogram of the earthquake.

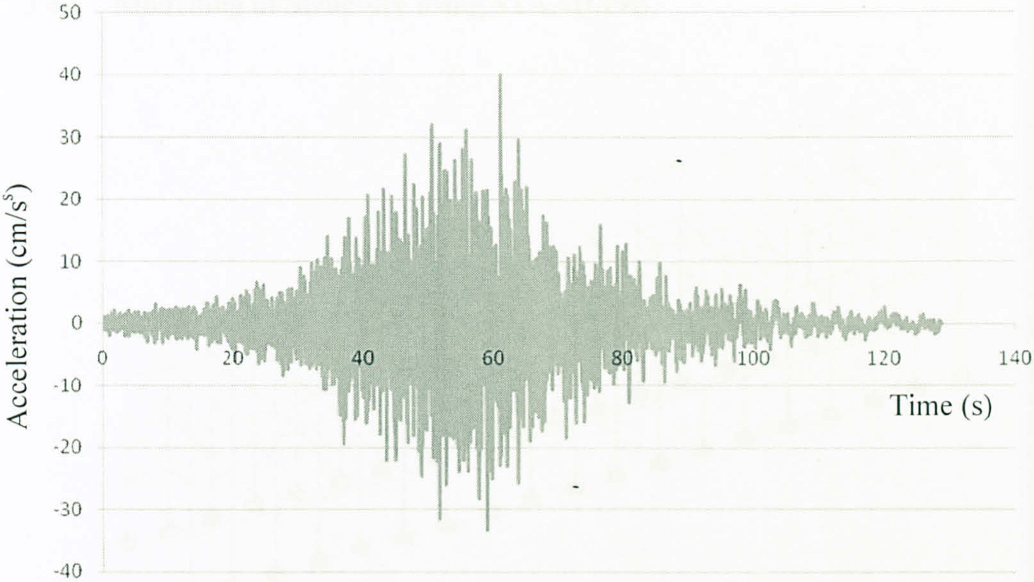

Figure 3.13. Seismogram of earthquake recorded at the Sikuai Island station, West Sumatra

The seismogram is made up of 25,799 data points with acceleration ranges from -33.368cm/s^2 to 40.017cm/s^2. The duration of earthquake recorded is approximately 129 seconds.

3.4 Analysis of Time-History Response of Structure

Using the time-history data of 2007 Sumatra earthquake, the school structure is modelled in STAAD.Pro, and the seismic load is imposed on the structure. The results of the analysis are reported in Chapter 4.

3.4.1 Modelling of Structure using STAAD.Pro

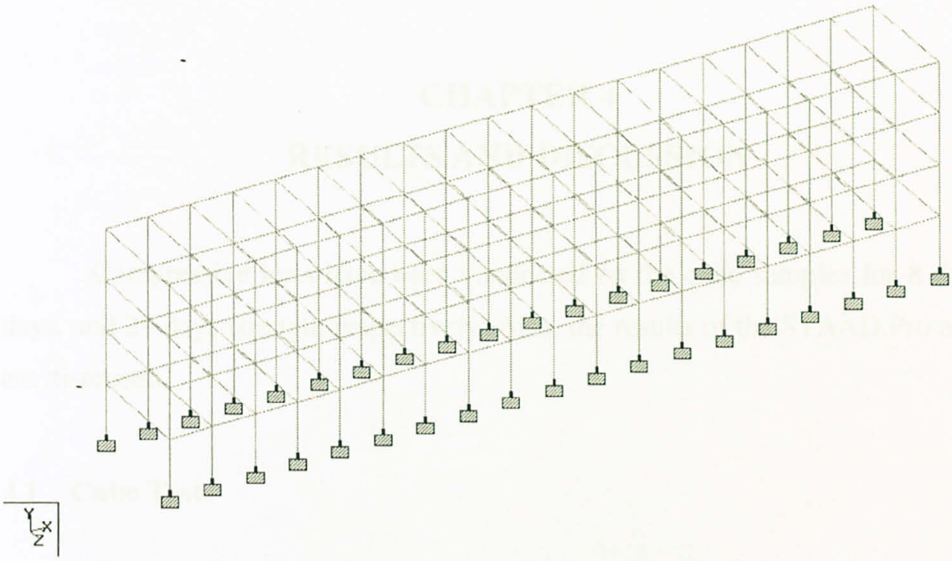

Figure 3.14. Model of school building in STAAD.Pro.

This model is 3 storeys in total (including foundation column), supported by 38 columns on each floor, and has a total of 372 beams (refer Figure 3.14). All column bases are assigned as fixed supports. The roof beams are assigned dimensions of 600mm x 150mm, while the other floor beams have dimensions of 550mm x 150mm. The beams had lengths of 3m (spanning from one column to the adjacent column) and 7.8m (spanning from one column to the opposite column). The columns have equal dimensions for each floor, which is 250mm x 350mm. The height of each column was 3.6m. The material assigned for the model is concrete, which has density of $23.6kN/m^3$. The Young's Modulus (E) is 21.7GPa. In an actual structure, there exists damping. Therefore, this model has also been assigned a critical damping coefficient of 0.05.

For the load cases, the model was assigned a dynamic load case. Self weight of the structure was considered in the X, Y and Z direction, with a factor of 1.0. For each of the floors (except ground floor), a distributed load of $1.5kN/m^2$ was also assigned in the X, Y, and Z direction. The time-history of the Sumatra earthquake selected earlier is then input into the software. The inputs required are the time (seconds) and the corresponding acceleration (meter/second/second).

CHAPTER 4
RESULTS AND DISCUSSION

Compressive tests have been conducted on the cube samples for 8 days, 14 days, and 29 days strength respectively. Also, the results of the STAAD.Pro analysis are discussed.

4.1 Cube Test

Compressive strength tests have been conducted on the cube samples for 8 days, 14 days, and 29 days to verify the designed concrete strength. Detailed information on the cube test results is shown in Appendix E. Table 4.1 shows the summary of the cube tests results.

Table 4.1. Results of compressive test on cube samples

Cubes / Days	Compressive strength (N/mm^2)		
	1	**2**	**3**
8	36.05	36.11	37.52
14	47.58	43.18	46.62
29	53.75	55.72	54.21

From the table, it can be seen that the concrete strength exceeds the design strength of $30N/mm^2$. Comparing the result shows slight variation due to the nature of concrete which is a variable material, having a wide range of strengths and stress-strain behaviour. (Mosley, 1999). It is also observed that the concrete far exceeds the design strength. This may be due to the type of cement being used in the concreting process, which may have contained admixtures that would enhance the concrete strength. Figure 4.1 shows the concrete hardening process.

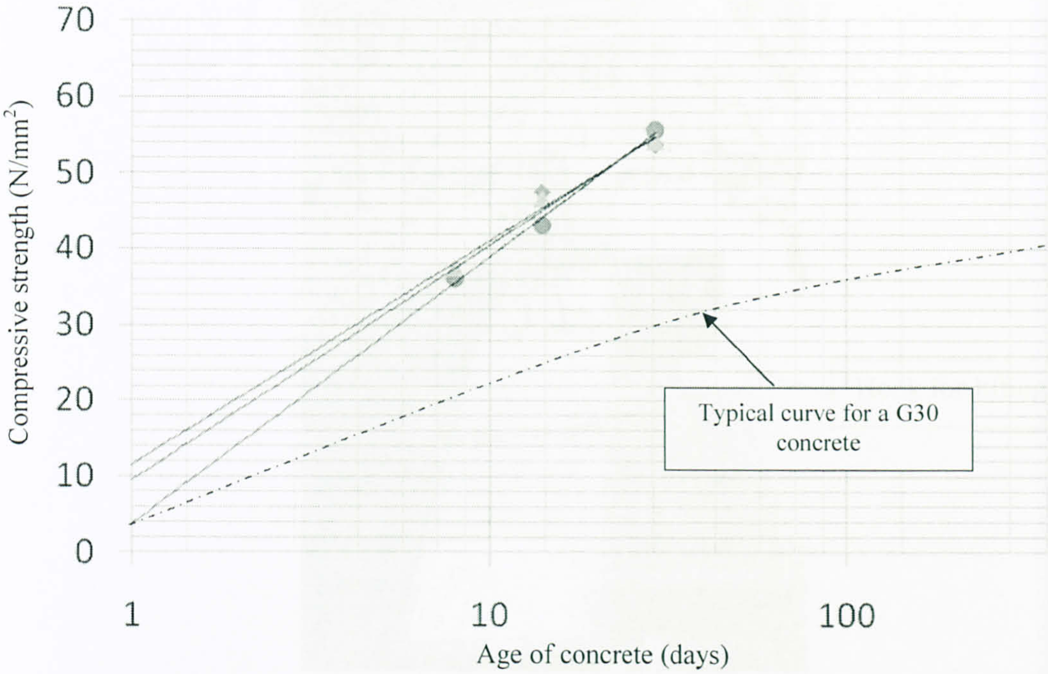

Figure 4.1. Increase of concrete strength with age.

With the increase in concrete strength, the joint capacity is expected to be higher than the initial estimate. However, this assumption can only be verified by conducting the actual experiment.

4.2 Experimental works

For this experiment, the concrete joint samples, steel supports and testing jig were outsourced from a local contractor. Figures 4.2 and 4.3 show the actual items that have been fabricated.

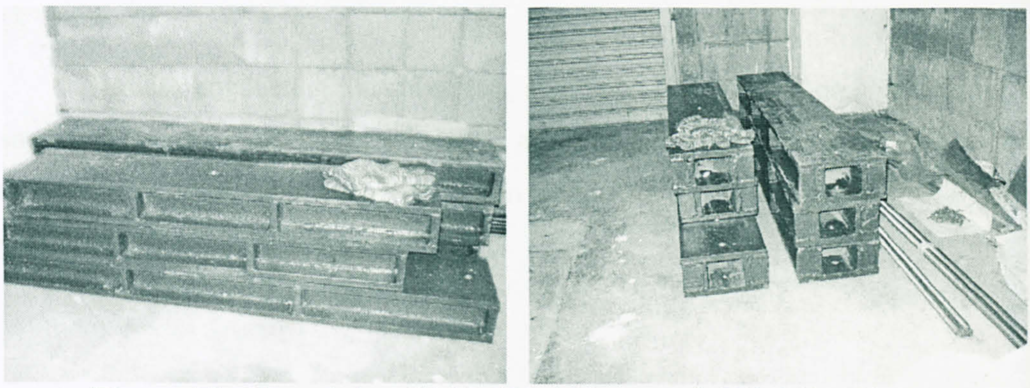

Figure 4.2. Plate girders (1255x200x100mm and 975x200x100mm)

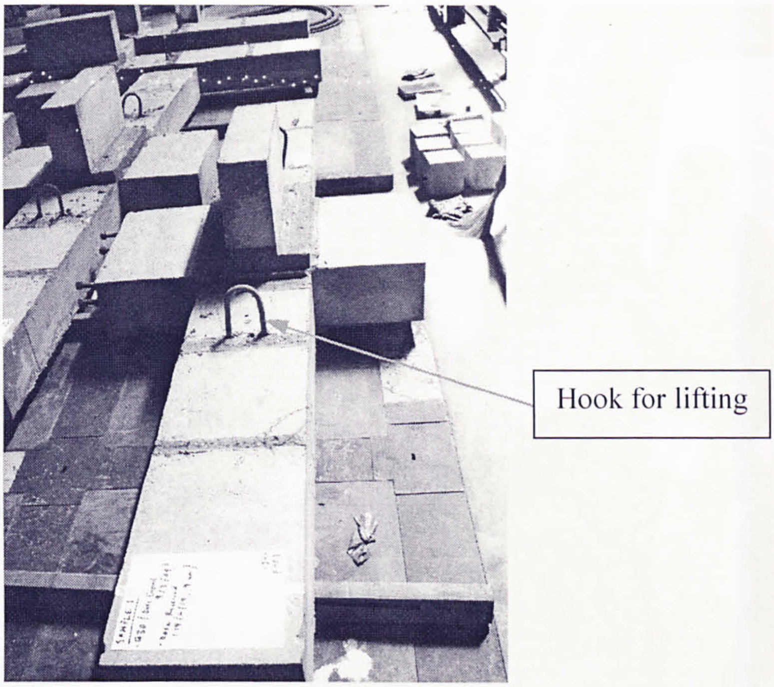

Figure 4.3. Concrete joint sample

Figure 4.4 shows the fracture on the concrete cubes after testing. None of the cubes exhibited explosive failure pattern.

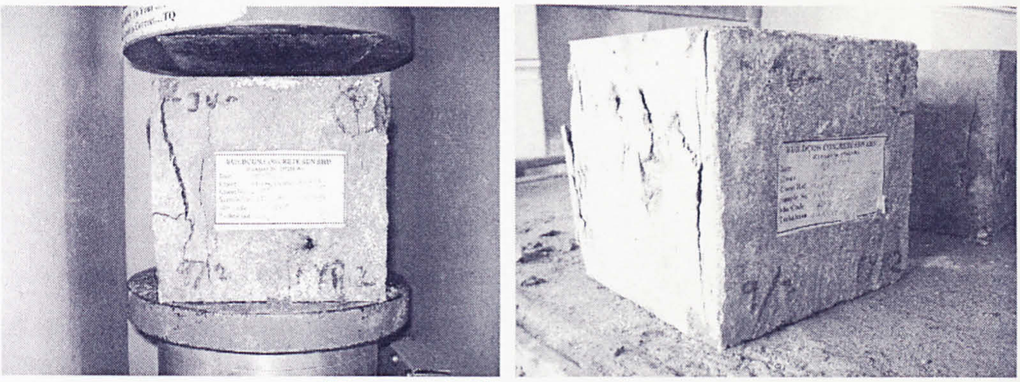

Figure 4.4. Concrete cube test

Besides conducting the cube tests, some pre-experimental preparations were such as lifting and positioning of sample and supports, demarcation of gridlines on the concrete joint, and fixing of strain gauges. Figures 4.5 to 4.7 show the preparation done to the samples.

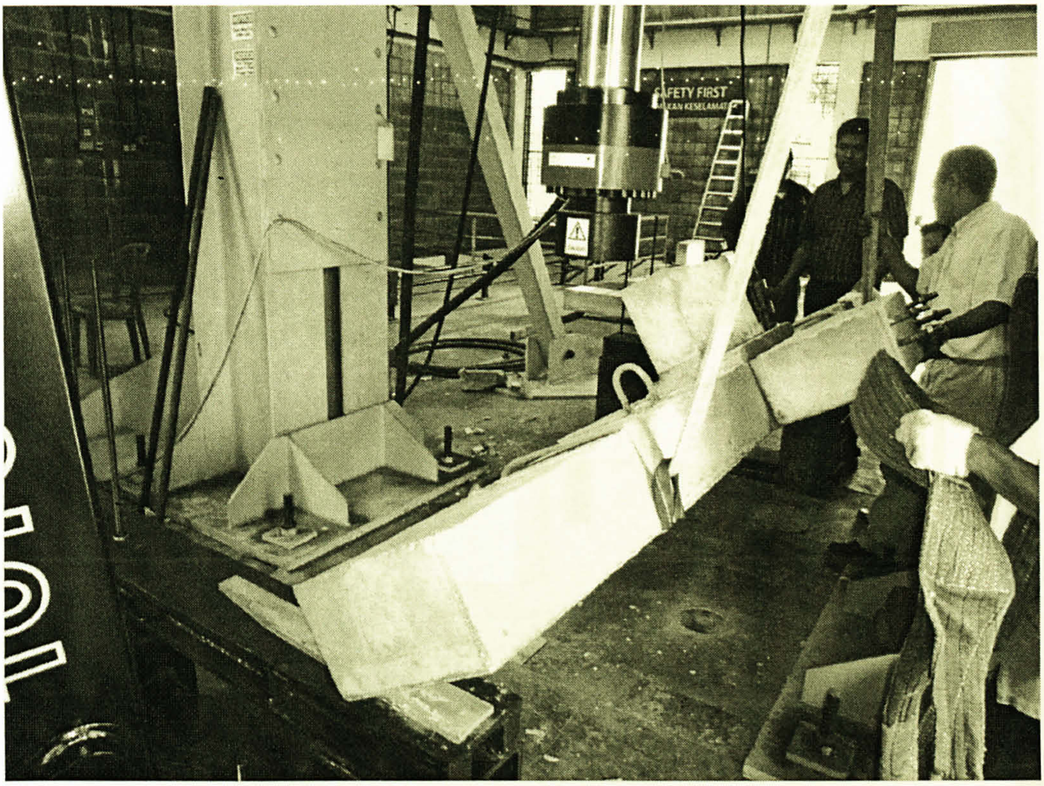

Figure 4.5. Lifting and positioning of joint sample.

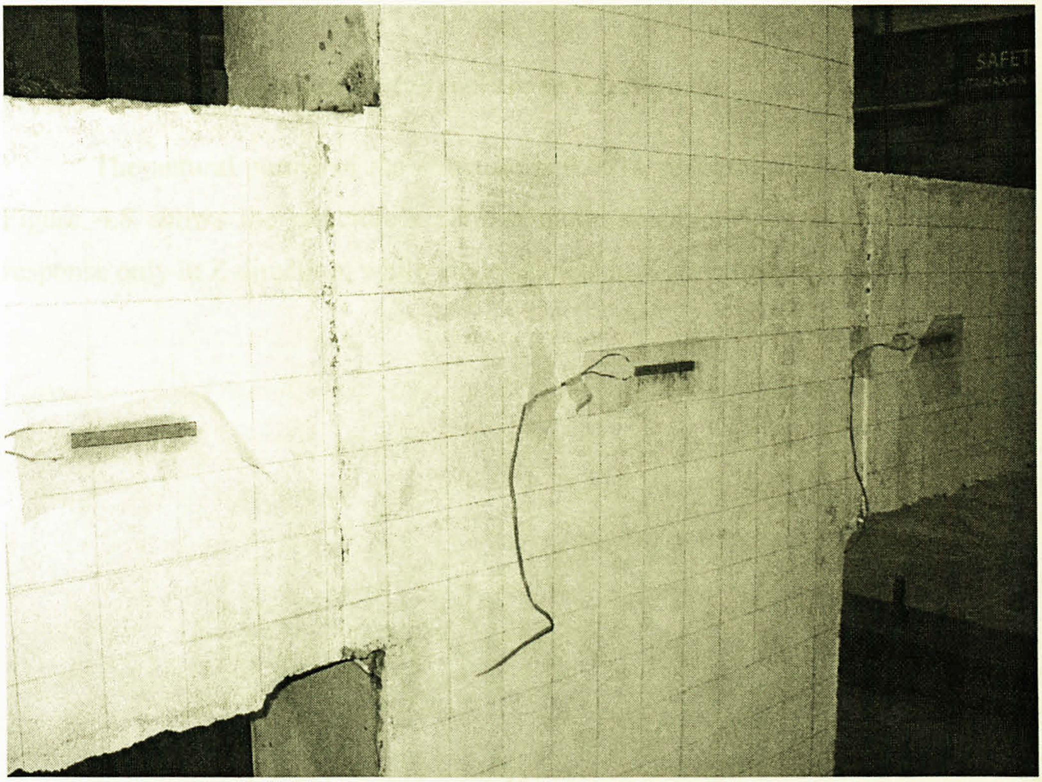

Figure 4.6. Gridlines at 50mm x 50mm spacing and strain gauges.

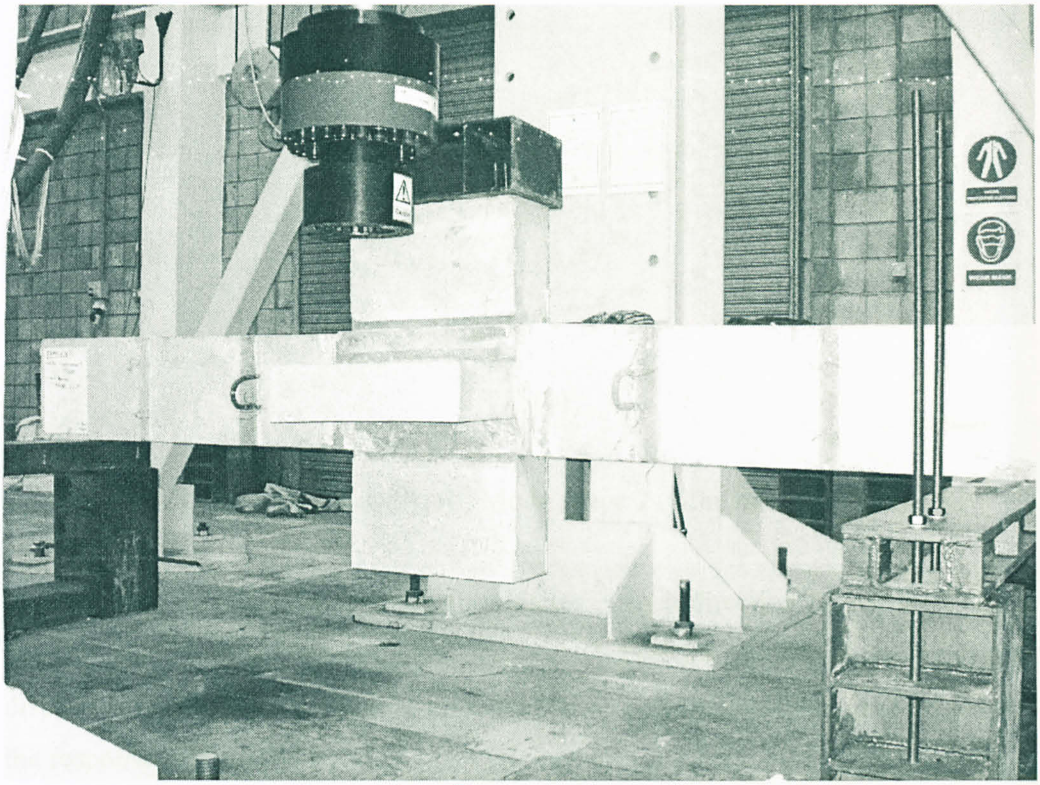

Figure 4.7. Final experimental setup

4.3 Time-history Response of Structure to Earthquake

The natural period of the structure is 0.691s, as obtained from STAAD.Pro. Figure 4.8 shows the structure's various mode shapes. Mode shape 1 gives the response only in Z-direction, while mode shape 2 in X-direction.

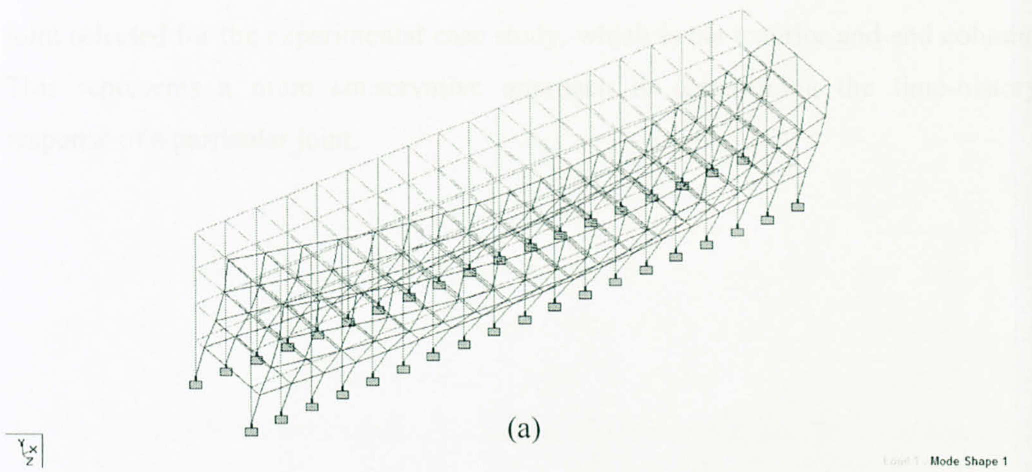

(a)

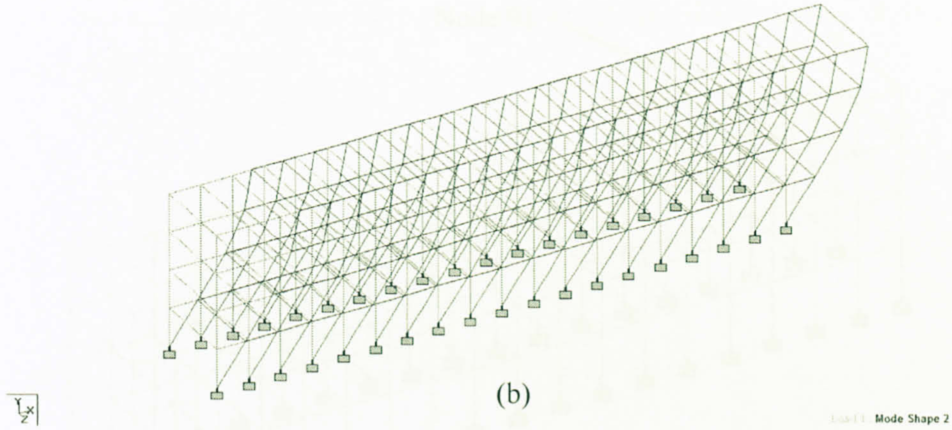

(b)

Figure 4.8. (a) Mode shape 1; (b) Mode shape 2 of the model after analysis.

Table 4.2 shows the participation factor in each direction for modes 1 and 2. Mode 1 has the largest participation factor in Z-direction (81%), where the largest displacement occurs in the similar direction. It can be concluded that mode 1 governs the response of the building.

Table 4.2. Participation Factor for Each Mode.

Mode	Frequency (Hz)	Period (s)	Participation X (%)	Participation Y (%)	Participation Z (%)
1	1.447	0.691	0.000	0.000	80.929
2	1.456	0.687	88.992	0.000	0.000

Node 91 (refer Figure 4.9), which had the largest displacement amplitude was selected to obtain its time-history response. This was in contrary to the actual joint selected for the experimental case study, which is the exterior and end column. This represents a more conservative approach in determining the time-history response of a particular joint.

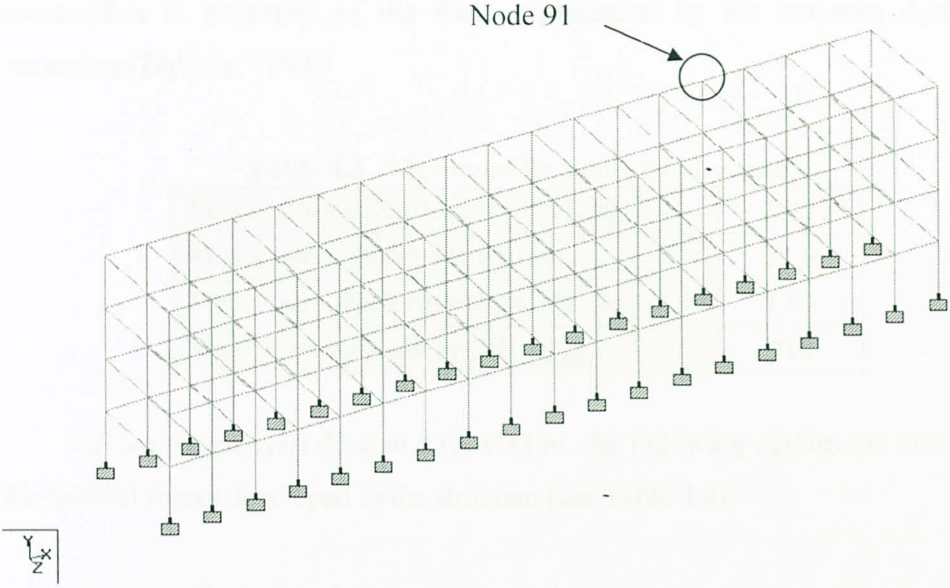

Figure 4.9. Time-history displacement response of joint subjected to Sumatra earthquake.

Figure 4.10 shows the time-history response of the node 91 as obtained from STAAD.Pro, for displacement in Z-direction.

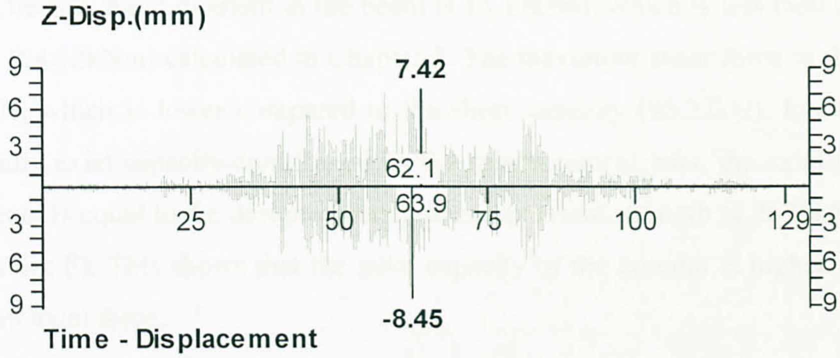

Figure 4.10. Time-history displacement response of joint subjected to Sumatra earthquake.

The maximum responses for the earthquake specified (Sumatra, 2007) are summarized in Table 4.3. The maximum displacement of the structure under the given earthquake is 8.45mm, and the joint is located at the top floor. The displacement is important in the earthquake analysis because stresses in the structural members are directly proportional to the relative displacement. The absolute acceleration is indicative of the force experienced by the structure during the excitation (Tedesco, 1998).

Table 4.3. Maximum Response of Structure

Maximum displacement (mm), x_{max}	8.45
Maximum velocity (mm/s), $\dot{x}_{max}$	73.6
Maximum acceleration (m/ s²), $\ddot{x}_{max}$	1.03
Maximum base shear (kN), V_{max}	218

From the analysis done in STAAD.Pro, the following outputs are obtained as the internal forces developed in the structure (see Table 4.4).

Table 4.4. Maximum Forces in Members of Structure

		Axial Force (kN)	**Shear Force (kN)**	**Moment (kNm)**
Beam (550x150mm)	**max**	0.716	4.66	18.17
	min	-0.716	-4.51	-18.17
Column (250x350mm)	**max**	12.3	6.30	13.76
	min	-12.3	-6.09	-14.23

The maximum moment in the beam is 18.17kNm, which is less than the joint capacity (64.52kNm) calculated in Chapter 3. The maximum shear force in the beam is 4.66kN, which is lower compared to the shear capacity (95.22kN). Ignoring the additionally axial capacity contributed by the reinforcement bars, the axial capacity of the beam is equal to the designed concrete compressive strength of 2625kN (Refer to Appendix F). This shows that the axial capacity of the column is higher than the maximum axial force.

As the internal forces of the members are less than its capacity, the structure is expected to be safe from the earthquake with the same or less in magnitude with the 2007 Sumatra earthquake. The time-history response can also be used to calculate the fatigue of the structure in the experimental work.

CHAPTER 5

CONCLUSION AND RECOMMENDATION

This project is a pre-experimental study to investigate the effect of an earthquake on building joints. Building joint failure is one of the main causes of structural failure. In this project, a school building is selected as the case study. An exterior joint is chosen and samples of it are fabricated. With the joint samples fabricated, the objective of this project is to design an experimental setup for the testing of the joints. In addition, software analysis using STAAD.Pro is done to obtain a theoretical implication of the earthquake on the joint.

The design of experimental setup involved surveying laboratory facilities, reinforced concrete and steel design according to BS 8110 and BS 5950, fabrication and modification works, planning, and procurement.

From the STAAD.Pro output, it can be summarized that the maximum joint displacement that can occur is 8.45mm. This value is a linear indication of the stresses that can occur in the structural members. Comparing the maximum forces in the members, it can be concluded that the joint has higher capacity and is expected to be safe from the earthquake of magnitude similar or lesser than the 2007 Sumatra earthquake.

As a conclusion, the preliminary ground works have been completed for this project and the next stage to be accomplished is conducting the experimental study. Further works that can be undertaken for the experimental study is fatigue analysis by using statistical methods such as rainflow cycle counting method.

There are many structural aspects which can be further investigated. Suggested future works which can be done are such as:-

- Experimental test on other types of RC joints and joints with different detailing.
- Experimental test on steel joint connections.
- Experimental test on retrofitted joints.

REFERENCES

Adnan, A. & Irsyam, M. (2002) The Effect of the Latest Sumatra Earthquake to Malaysian Peninsular. Journal of Civil Engineering Universiti Teknologi Malaysia, 15 (2), 1-12.

Ariduru, C. (2004) Fatigue Life Calculation by Rainflow Cycle Counting Method. M.Sc Thesis, Middle East Technical University, Turkey.

Bolt, B.A. (2003) Earthquakes: Fifth Edition. New York. W.H. Freeman and Company.

Campbell, S.D., et al. (2008) Steel Moment Frame Damage Predictions Using Low-Cycle Fatigue, *The 14th World Conference on Earthquake Engineering, Beijing, China*

Elwood, K.J. & Moehle, J.P. (2008) Dynamic Shear and Axial-Load Failure of Reinforced Concrete Columns. *Journal of Structural Engineering*, 134 (7), 1189-1198.

Erdey, C.K. (2006) Earthquake Engineering: application to design. New Jersey. John Wiley & Sons, Inc.

Lowes, L.N. & Altoontash, A. (2003) Modeling Reinforced-Concrete Beam-Column Joints Subjected to Cyclic Loading. *Journal of Structural Engineering,* 129 (12), 1686-1697.

Megawati, K. et al. (2005) Response spectral attenuation relationships for Sumatran-subduction earthquakes and the seismic hazard implications to Singapore and Kuala Lumpur. Soil Dynamics and Earthquake Engineering, 25, 11-25.

Mosley, W.H. et al. (1999) Reinforced Concrete Design: Fifth Edition. Houndmills. Palgrave.

Pantelides, C.P. et al. (2008) Seismic Rehabilitation of Reinforced Concrete Frame Interior Beam-Column Joints with FRP Composites. Journal of Composites for Construction, 12 (4), 435-445.

Tatsuo, O. (ed) (1997) Dynamic Analysis and Earthquake Resistant Design. Strong Motion and Dynamic Properties Volume 1. Rotterdam, A.A. Balkema Publishers.

Tedesco, J.W. et al. (1998) Structural Dynamics: Theory and Applications. Addison-Wesley.

U.S. Geological Survey, Earthquake Hazards Program (2000) <http://quake.usgs.gov/recent/helicorders/index.html>

Walraven, J. (1994) Rough Cracks Subjected to Earthquake Loading. Journal of Structural Engineering, 120 (5), 1510-1524.

Watson, S. and Park, R. (1994) Simulated Seismic Load Tests on Reinforced Concrete Columns. Journal of Structural Engineering, 120 (6)

APPENDIX

APPENDIX A

Modified Mercalli Scale

The Mercalli scale originated with the widely used simple ten-degree Rossi-Forel scale, which was revised by Italian volcanologist Giuseppe Mercalli in 1883 and 1902. The terms or *Mercalli scale* should not be used unless one really means the original ten-degree scale of 1902.

In 1902 the ten-degree Mercalli scale was expanded to twelve degrees by Italian physicist Adolfo Cancani. It was later completely re-written by German geophysicist August Heinrich Sieberg and became known as the **Mercalli-Cancani-Sieberg** (MCS) scale. The Mercalli-Cancani-Sieberg scale was later modified and published in English by Harry O. Wood and Frank Neumann in 1931 as the **Mercalli-Wood-Neuman** (MWN) scale. It was later improved by Charles Richter, the father of the Richter magnitude scale. The scale is known today as the **Modified Mercalli Scale** and commonly abbreviated **MM** or **Io**.

The lower degrees of the MM scale generally deal with the manner in which the earthquake is felt by people. The higher numbers of the scale are based on observed structural damage. The table below is a rough guide to the degrees of the *Modified Mercalli Scale*. The colors and descriptive names shown here differ from those used on certain shake maps in other articles.

Table A-1. Mercalli Intensity Scale

I. Instrumental	Not felt by many people unless in favorable conditions.
II. Feeble	Felt only by a few people at best, especially on the upper floors of buildings. Delicately suspended objects may swing.
III. Slight	Felt quite noticeably by people indoors, especially on the upper floors of buildings. Many do not recognize it as an earthquake. Standing motor cars may rock slightly. Vibration similar to the passing of a truck. Duration estimated.
IV. Moderate	Felt indoors by many people, outdoors by few people during the day. At night, some awakened. Dishes, windows, doors disturbed; walls make cracking sound. Sensation like heavy truck striking building. Standing motor cars rocked noticeably. Dishes and windows rattle alarmingly.
V. Rather Strong	
VI. Strong	Felt by all; many frightened and run outdoors, walk unsteadily. Windows, dishes, glassware broken; books off shelves; some heavy furniture moved or overturned; a few instances of fallen plaster. Damage slight.
VII. Very Strong	Difficult to stand; furniture broken; damage negligible in building of good design and construction; slight to moderate in well-built ordinary structures; considerable

	damage in poorly built or badly designed structures; some chimneys broken. Noticed by people driving motor cars.
VIII. Destructive	Damage slight in specially designed structures; considerable in ordinary substantial buildings with partial collapse. Damage great in poorly built structures. Fall of chimneys, factory stacks, columns, monuments, walls. Heavy furniture moved.
IX. Ruinous	General panic; damage considerable in specially designed structures, well designed frame structures thrown out of plumb. Damage great in substantial buildings, with partial collapse. Buildings shifted off foundations.
X. Disastrous	Some well built wooden structures destroyed; most masonry and frame structures destroyed with foundation. Rails bent.
XI. Very Disastrous	Few, if any masonry structures remain standing. Bridges destroyed. Rails bent greatly.
XII. Catastrophic	Total damage - Almost everything is destroyed. Lines of sight and level distorted. Objects thrown into the air. The ground moves in waves or ripples. Large amounts of rock may move position.

Richter Scale

The Richter magnitude of an earthquake is determined from the logarithm of the amplitude of waves recorded by seismographs (adjustments are included to compensate for the variation in the distance between the various seismographs and the epicenter of the earthquake). Because of the logarithmic basis of the scale, each whole number increase in magnitude represents a tenfold increase in measured amplitude; in terms of energy, each whole number increase corresponds to an increase of about 31.6 times the amount of energy released.

Events with magnitudes of about 4.6 or greater are strong enough to be recorded by any of the seismographs in the world, given that the seismograph's sensors are not located in an earthquake's shadow.

The following describes the typical effects of earthquakes of various magnitudes near the epicenter. This table should be taken with extreme caution, since intensity and thus ground effects depend not only on the magnitude, but also on the distance to the epicenter, the depth of the earthquake's focus beneath the epicenter, and geological conditions (certain terrains can amplify seismic signals).

Table A-2. Richter scale

Richter Magnitudes	Description	Earthquake Effects	Frequency of Occurrence
Less than 2.0	Micro	Microearthquakes, not felt.	About 8,000 per day
2.0-2.9	Minor	Generally not felt, but recorded.	About 1,000 per day
3.0-3.9	Minor	Often felt, but rarely causes damage.	49,000 per year (est.)
4.0-4.9	Light	Noticeable shaking of indoor items, rattling noises. Significant damage unlikely.	6,200 per year (est.)
5.0-5.9	Moderate	Can cause major damage to poorly constructed buildings over small regions. At most slight damage to well-designed buildings.	800 per year
6.0-6.9	Strong	Can be destructive in areas up to about 160 kilometres (100 mi) across in populated areas.	120 per year
7.0-7.9	Major	Can cause serious damage over larger areas.	18 per year
8.0-8.9	Great	Can cause serious damage in areas several hundred miles across.	1 per year
9.0-9.9	Great	Devastating in areas several thousand miles across.	1 per 20 years
10.0+	Epic	Never recorded; see below for equivalent seismic energy yield.	Extremely rare (Unknown)

Table A-3 shows the comparison between the Modified Mercalli scale and the Richter scale

Table A-3. Non-numerical comparison between Mercalli Intensity Scale and Richter Scale

Mercalli Intensity Scale	Richter Scale
I	<3.5
II	3.5
III	4.2
IV	4.5
V	4.8
VI	5.4
VII	6.1
VIII	6.5
IX	6.9
X	7.3
XI	8.1
XII	>8.1

APPENDIX B

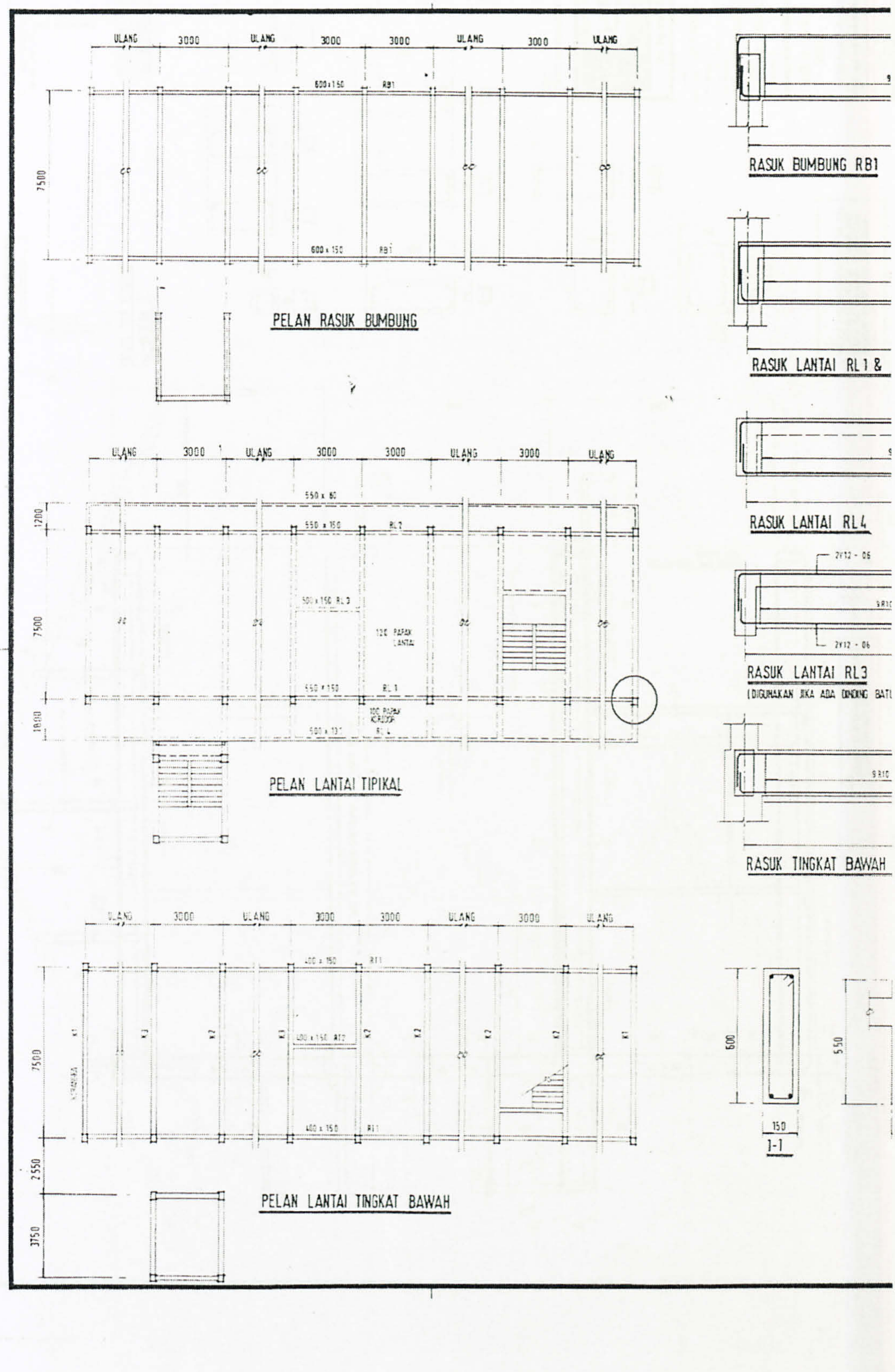
PELAN RASUK BUMBUNG
PELAN LANTAI TIPIKAL
PELAN LANTAI TINGKAT BAWAH
RASUK BUMBUNG RB1
RASUK LANTAI RL1 &
RASUK LANTAI RL4
RASUK LANTAI RL3
RASUK TINGKAT BAWAH
ULANG
3000
7500
1700
1800
2550
3750
600
550
150
1-1
600 x 150
RB1
550 x 150
RL 2
RL 1
400 x 150
RT1
2Y12 - D6

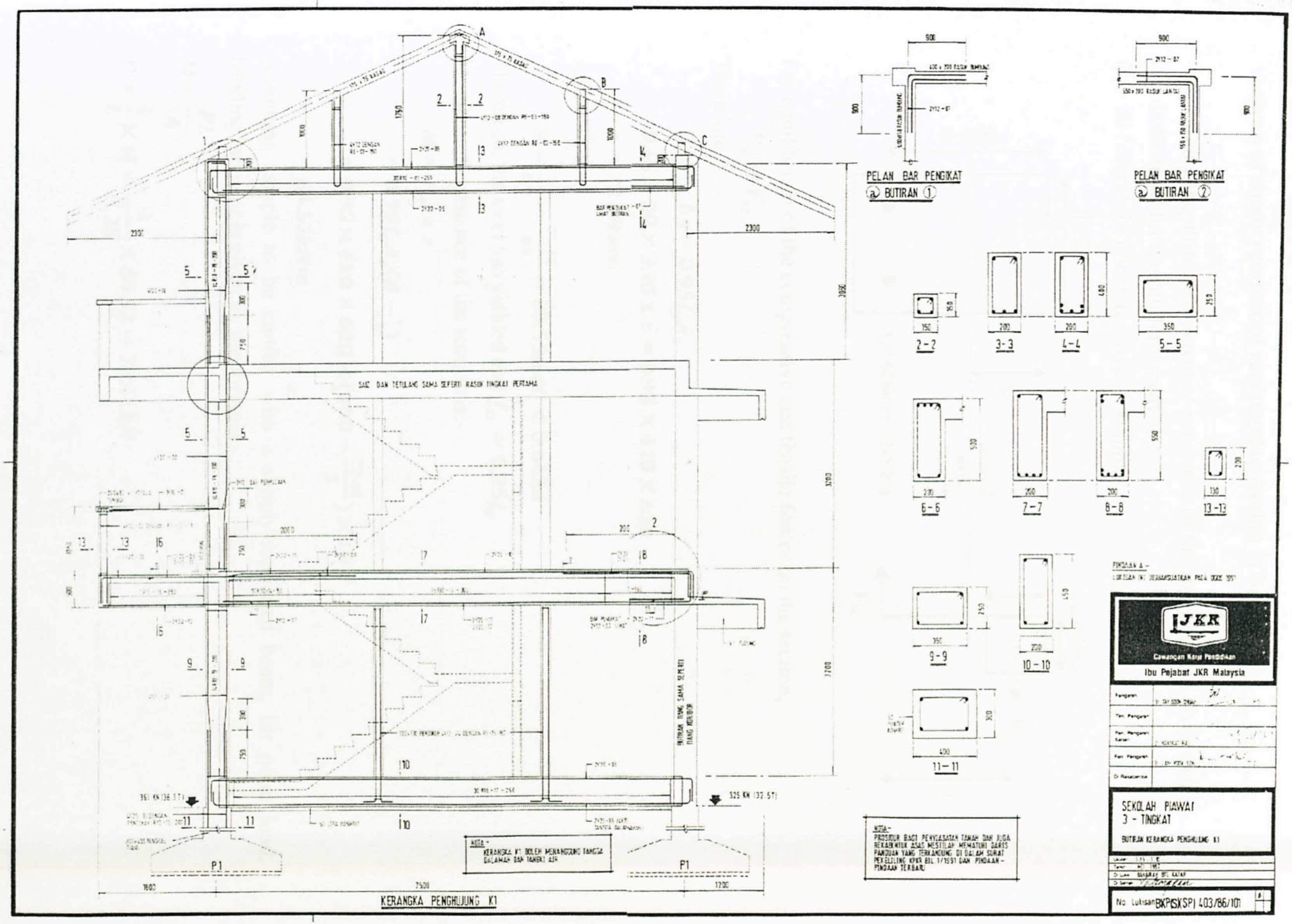
KERANGKA PENGHUJUNG K1
SAIZ DAN TETULANG SAMA SEPERTI RASUK TINGKAT PERTAMA
BUTIRAN RONG SAMA SEPERTI RANG KORIDOR
NOTA -
KERANGKA K1 BOLEH MENANGGUNG TANGGA DALAMAN DAN TANGKI AIR
P1
P1
361 KN (36.3 T)
525 KN (32.5T)
2300
2300
7500
1800
1700
PELAN BAR PENGIKAT
@ BUTIRAN ①
PELAN BAR PENGIKAT
@ BUTIRAN ②
2-2
3-3
4-4
5-5
6-6
7-7
8-8
13-13
9-9
10-10
11-11
NOTA -
PROSIDUR BAGI PENYIASATAN TANAH DAN JUGA REKABENTUK ASAS MESTILAH MEMATUHI GARIS PANDUAN YANG TERKANDUNG DI DALAM SURAT PEKELILING KPKR BIL 1/1991 DAN PINDAAN - PINDAAN TERBARU
PINDAAN A -
Cawangan Kerja Pendidikan
Ibu Pejabat JKR Malaysia
Pengarah
Tim. Pengarah
Pen. Pengarah Kanan
Pen. Pengarah
Di Rekabentuk
SEKOLAH PIAWAI
3 - TINGKAT
BUTIRAN KERANGKA PENGHUJUNG K1
No. Lukisan BKP(SKSP) 403/86/101

APPENDIX C

Analysis of singly reinforced rectangular section in bending

Determining the ultimate moment of resistance of the cross-section given that:-
f_y = **410N/mm²** for the reinforcement and;
f_{cu} = 30 N/mm² for concrete, cover = 40mm

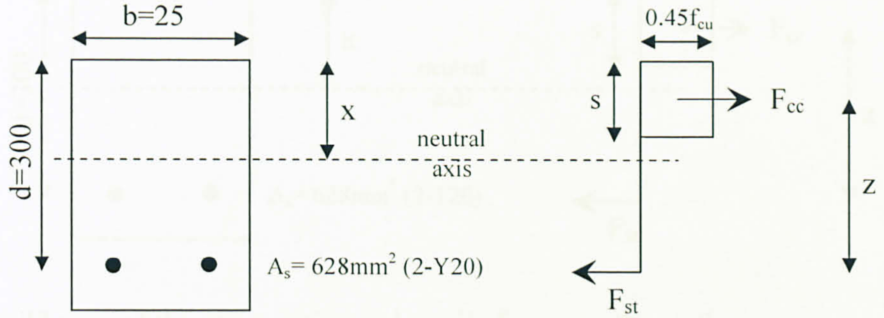

For equilibrium of the compressive and tensile forces on the section,

$$F_{cc} = F_{st}$$

Therefore,

$$0.45 f_{cu} bs = 0.95 f_y A_s$$

$$0.45 \times 30 \times 250 \times s = 0.95 \times 410 \times 628$$

$$s = 72.48mm$$

And

$$x = \frac{s}{0.9} = \frac{72.48}{0.9} = 80.53mm \ < 0.642d$$

Therefore, the steel has yielded and $f_{st} = 0.95 f_y$

Moment of resistance of the section is:-

$$M = F_{st} \times z$$

$$= 0.95 f_y A_s \left(d - \frac{s}{2}\right)$$

$$= 0.95 \times 410 \times 628 \times \left(300 - \frac{72.48}{2}\right) \times 10^{-6}$$

$$= 64.52kNm$$

Assuming sample to be similar with a simply-supported beam, for point load, bending moment is given by the formula:-

$$M = \frac{PL}{4}$$

$$P = \frac{4}{L} \times M = \frac{4}{3.25} \times 64.52 = 79.41kN$$

Analysis of singly reinforced rectangular section in bending

Determining the ultimate moment of resistance of the cross-section given that:-
f_y = **460N/mm²** for the reinforcement and;
f_{cu} = 30 N/mm² for concrete, cover = 40mm

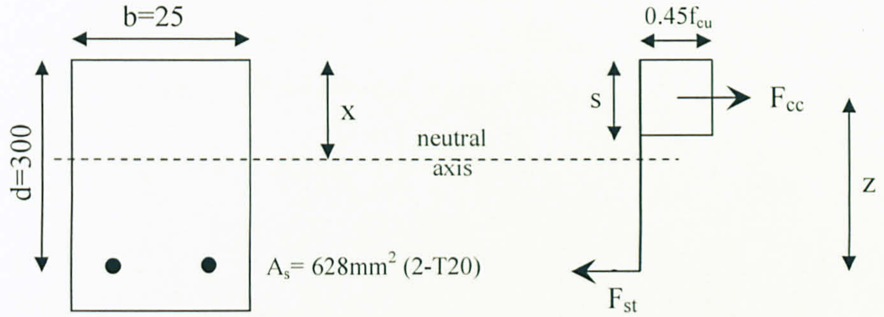

For equilibrium of the compressive and tensile forces on the section,

$$F_{cc} = F_{st}$$

Therefore,

$$0.45 f_{cu} bs = 0.95 f_y A_s$$

$$0.45 \times 30 \times 250 \times s = 0.95 \times 460 \times 628$$

$$s = 81.31mm$$

And

$$x = \frac{s}{0.5} = \frac{81.31}{0.5} = 90.34mm < 0.615d$$

Therefore, the steel has yielded and $f_{st} = 0.95 f_y$

Moment of resistance of the section is:-

$$M = F_{st} \times z$$

$$= 0.95 f_y A_s (d - \frac{s}{2})$$

$$= 0.95 \times 460 \times 628 \times (300 - \frac{81.31}{2}) \times 10^{-6}$$

$$- 71.17kNm$$

Assuming sample to be similar with a simply-supported beam, for point load, bending moment is given by the formula:-

$$M = \frac{PL}{4}$$

$$P = \frac{4}{L} \times M = \frac{4}{3.25} \times 71.17 = 87.59kN$$

Analysis of singly reinforced rectangular section in bending

Determining the ultimate moment of resistance of the cross-section given that:-

f_y = **500N/mm²** for the reinforcement and;

f_{cu} = 30 N/mm² for concrete, cover = 40mm

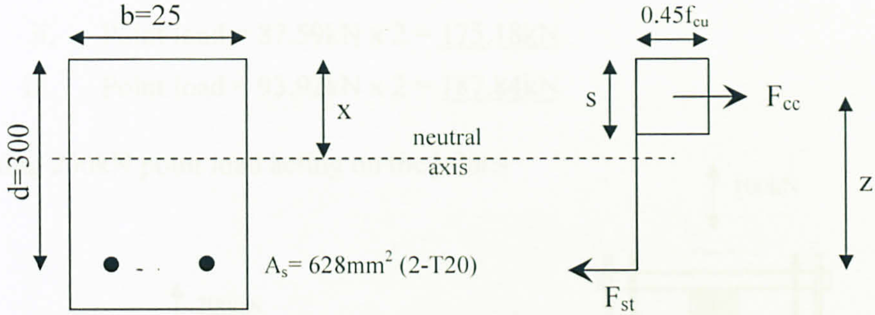

For equilibrium of the compressive and tensile forces on the section,

$$F_{cc} = F_{st}$$

Therefore,

$$0.45 f_{cu} bs = 0.95 f_y A_s$$

$$0.45 \times 30 \times 250 \times s = 0.95 \times 500 \times 628$$

$$s = 88.39mm$$

And

$$x = \frac{s}{0.5} = \frac{88.39}{0.5} = 98.21mm \ < 0.595d$$

Therefore, the steel has yielded and $f_{st} = 0.95 f_y$

Moment of resistance of the section is:-

$$M = F_{st} \times z$$

$$= 0.95 f_y A_s (d - \frac{s}{2})$$

$$= 0.95 \times 500 \times 628 \times (300 - \frac{88.39}{2}) \times 10^{-6}$$

$$- 76.31kNm$$

Assuming sample to be similar with a simply-supported beam, for point load, bending moment is given by the formula:-

$$M = \frac{PL}{4}$$

$$P = \frac{4}{L} \times M = \frac{4}{3.25} \times 76.31 = 93.92kN$$

APPENDIX D

Estimating loading for the design of plate girder

Taking a safety factor of 2,

i. Point load = 79.41kN x 2 = 158.82kN

ii. Point load = 87.59kN x 2 = 175.18kN

iii. Point load = 93.92kN x 2 = 187.84kN

Assuming 200kN point load acting on the joint:-

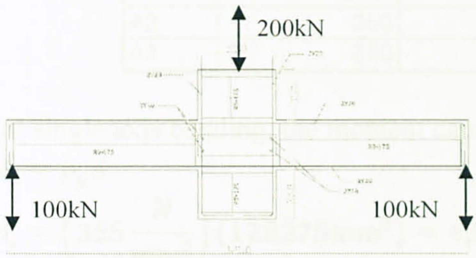

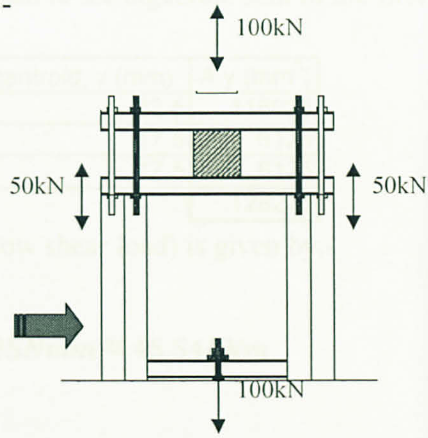

To determine the moment imposed on the *1255mm x 200mm x 100mm* plate girder:-

$$M = \frac{PL}{4} = \frac{(100kN)(1.255m)}{4}$$

$$M = \underline{\underline{31.375kNm}}$$

→Therefore, the design of the plate girder should sustain an imposed moment of 31.375kNm.

To determine the imposed moment on the *975mm x 200mm x 100mm* plate girder:-

$$M = \frac{PL}{4} = \frac{(100kN)(0.975m)}{4}$$

$$M = \underline{\underline{24.375kNm}}$$

→Therefore, the design of the plate girder should sustain an imposed moment of 24.375kNm.

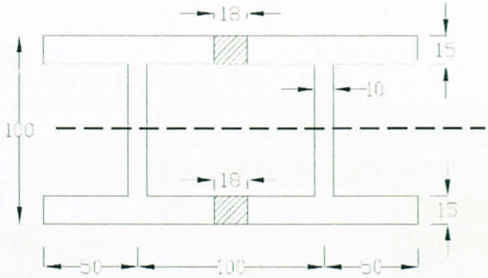

Figure 1. Cross-section of 1255mm x 200mm x 100mm plate girder

Given that the plastic modulus of a section is equal to the algebraic sum of the first moments of area about the equal area axis,

Region	Area, A (mm^2)	Distance to centroid, y (mm)	A.y (mm^3)
A1	2730	42.5	116025
A2	350	17.5	6125
A3	350	17.5	6125
			128275

For single axis bending, the moment capacity (low shear load) is given by:-

$$M_c = p_y S$$

$$M_c = \left(355\frac{N}{mm^2}\right)(128275mm^3) = 45537625Nmm \approx 45.54kNm$$
$$> 31.375kNm$$

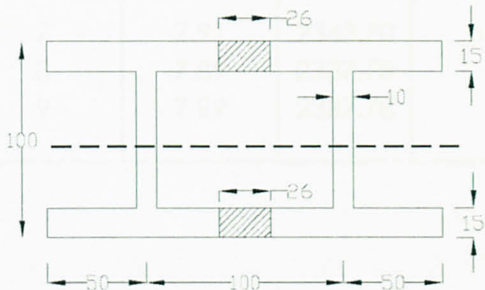

Figure 2. Cross section of 975mm x 200mm x 100mm plate girder

Given that the plastic modulus of a section is equal to the algebraic sum of the first moments of area about the equal area axis,

Region	Area, A (mm^2)	Distance to centroid, y (mm)	A.y (mm^3)
A1	2610	42.5	110925
A2	350	17.5	6125
A3	350	17.5	6125
			123175

For single axis bending, the moment capacity (low shear load) is given by:-

$$M_c = p_y S$$

$$M_c = \left(355\frac{N}{mm^2}\right)(123175mm^3) = 43727125Nmm \approx 43.73kNm$$
$$> 24.375kNm$$

APPENDIX E

Concrete Cube Testing

Concrete supplier	Buildcon Concrete Sdn. Bhd.			
Client	Civil Engineering Department, Universiti Teknologi PETRONAS			
Concrete grade	30		**Casting date**	9/2/2009
Cube dimensions	**Width (mm)**	150	**Total No. of Cubes**	9
	Length (mm)	150	**Nominal aggregate size (mm)**	20
	Height (mm)	150		

Concrete age (days)	Date/Time	Cube No.	Weight (kg)	Density (kg/m³)	Loading rate (kN/s)	Maximum Peak Load (kN)	Sample stress (N/mm²)	Teste by
8	17/2/2009 (Tuesday) 12.20pm	1	7.97	2361.48	6.8	811.1	36.05	
		2	7.95	2355.56		812.6	36.12	VCC
		3	7.99	2367.41		844.2	37.52	
14	23/2/2009 (Monday) 10.30am	4	8.02	2376.30	6.8	1071	47.60	
		5	7.92	2346.67		971.6	43.18	VCC
		6	8.06	2388.15		1044	46.40	
29	10/3/2009 (Tuesday) 12.45pm	7	7.91	2343.70	6.8	1209	53.73	
		8	7.89	2337.78		1254	55.73	VCC
		9	7.89	2337.78		1220	54.22	

APPENDIX F

Determining shear capacity of the column

For the 9mm diameter shear links, $A_{sv} = 63.6mm^2$

$$\frac{A_{sv}}{s_v} = \frac{2 \, x \, 63.6}{175} = 0.727$$

The ultimate shear stress, v_c (for concrete strength of $f_{cu} = 30 \text{ N/mm}^2$) = 0.579N/mm^2

Therefore, the shear resistance of concrete plus shear links is given by:-

$$V_n = \left(\frac{A_{sv}}{s_v} 0.95 f_{yv} + b v_c\right) d$$

$$V_n = (0.727 \, x \, 0.95 \, x \, 250 + \ 250 \, x \, 0.579) 300$$

$$V_n = (0.727 \, x \, 0.95 \, x \, 250 + \ 250 \, x \, 0.579) 300$$

$$V_n = 95223.75N \approx 95.22kN$$

Determining axial capacity of the column

Axial capacity = Concrete strength x Cross section area of column
= 30 N/mm^2 x 250mm x 350mm
= 2625kN